Energy Conversion and Management 286 (2023) 117059

Contents lists available at ScienceDirect

Energy Conversion and Management

journal homepage: www.elsevier.com/locate/enconman

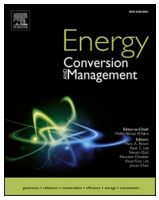

Green hydrogen from solar power for decarbonization: What will it cost?

Sushant S. Garud, Fanlok Tsang, Iftekhar A. Karimi [1,*], Shamsuzzaman Farooq [1]

Department of Chemical & Biomolecular Engineering, National University of Singapore, 4 Engineering Drive 4, Singapore 117585, Singapore

ARTICLE INFO

Keywords:
LCOH
Green hydrogen
Battery
Solar
Optimal design
Technoeconomic analysis

ABSTRACT

Green hydrogen has been touted as the silver bullet for deep decarbonization. For green hydrogen to become a reality, its production must be economically competitive and practically scalable. Much effort is being devoted towards enhancing technologies such as water electrolysis, battery storage, and hydrogen storage. In this work, a detailed optimization model for designing a green hydrogen production facility with minimum landed cost of hydrogen is presented. The model is employed to study green hydrogen production in Saudi Arabia, Australia, Singapore, and Germany and to highlight the impact of geospatial solar irradiance on the facility design. The least production cost of \$10.68 /kg-H_2 occurs in Saudi Arabia based on the current technoeconomic landscape. The analyses highlight that storing hydrogen molecules in tanks is more economical than storing renewable electrons in batteries for producing green hydrogen. Grid-connected green hydrogen production facilities may yield lower hydrogen production cost but cannot guarantee carbon-free hydrogen. The sensitivity analyses with respect to a few technoeconomic factors highlight that massive reductions in solar panel and battery costs combined with low-interest loan incentives can make green hydrogen cost competitive. Overall, this work offers the research and industry communities a versatile and powerful tool to study the evolving technoeconomic landscape of green hydrogen production.

1. Introduction

Several developing nations and emerging economies around the globe are aspiring to become developed nations and mature economies. Moreover, the global population has been rising and is expected to grow steadily over the coming decades. These two factors translate into rising global energy demands across various sectors such as power, industry, and transport. Besides small contributions from renewable resources, the current global energy mix continues to be dominated by fossil fuels and their derivatives. Many nations and regions [USA [1], Europe [2], Latin America [3], China [4], and Singapore [5]] across the globe are converging to the urgent need for carbon management and eventual need for deep decarbonization. This growing impetus coupled with the geopolitical dynamics surrounding the conventional energy resources (coal, oil, natural gas, etc.) are compelling researchers, industries, and nations all over the world to explore sustainable, low/no carbon energy options. A highly sought-after option is to transition from the current oil and gas-based economy to hydrogen-based economy [6]. The global interest in a hydrogen economy is evident from the efforts of several developed and developing nations, multi-national corporations, think tanks, and research institutions [7].

Currently, the large-scale use of hydrogen is limited to oil refineries, and in the production of methanol and ammonia. However, hydrogen economy goes beyond these conventional applications and deems hydrogen as an energy vector targeted towards industrial heating, power generation, and fueling transport sectors. Several studies exist in the literature discussing the role of different types of hydrogen in decarbonizing the industry [8], power [8], transport [9], and marine sectors [10]. Conventionally, steam reforming of natural gas [11] has been the main hydrogen production route. While this can be augmented with carbon capture and sequestration (CCS) to produce blue hydrogen, economic production of green hydrogen (GH_2) is the long-term objective for deep decarbonization in hydrogen economy. In this work, the scope is limited to GH_2, thus other types of hydrogen (such as grey, blue, purple, orange, etc.) and the associated literature is not discussed. Interested readers may refer to extensive exposition by Ishaq et al. [12] on the production and utilization of various types of hydrogen.

Thermochemical cycles, biomass gasification, and water electrolysis [13] are currently the main technologies for producing carbon-free hydrogen. Thermochemical cycles utilize chemical reactions driven by heat to decompose water. However, they are still in the developmental

* Corresponding author.
E-mail address: cheiak@nus.edu.sg (I.A. Karimi).
[1] The two authors have the same contribution to this study.

https://doi.org/10.1016/j.enconman.2023.117059
Received 20 October 2022; Received in revised form 19 March 2023; Accepted 13 April 2023
Available online 23 April 2023

Nomenclature

Acronyms

ACAPEX	Annualized Capital Expenditure
ALE	Alkaline Electrolysis
ATAF	Advanced Technology Advancement Factor
AUS	Australia
BS	Battery Storage
BSS	Battery Storage System
BST	Battery Storage Technology
BU1	Battery Unit Type 1
BU2	Battery Unit Type 2
CAPEX	Capital Expenditure
CCS	Carbon Capture and Sequestration
CI	Carbon Intensity
DF	Discount Factor
FEED	Front-End Engineering Design
FGE	Facility with Grid Export
FGI	Facility with Grid Import
FGIE	Facility with Grid Import and Export
FOPEX	Fixed Operating Expense
GER	Germany
GH_2	Green Hydrogen
ILF	Islanded Facility
KSA	Saudi Arabia
LCOE	Levelized Cost of Electricity
LCOH	Landed Cost of Hydrogen
LFP	Land Footprint
PEM	Polymer Electrolyte Membrane
PV	Photovoltaic
PVT	PV Technology
SIN	Singapore
SOE	Solid Oxide Electrolysis
SPV1	Solar PV Panel Type 1
SPV2	Solar PV Panel Type 2
TAC	Total Annualized Cost
TOC	Total Ownership Cost
TPD	Tonne Per Day
TPH	Tonne Per Hour
TRL	Technology Readiness Level
WE	Water Electrolysis
WEP	Water Electrolysis Plant
WET	WE Technology

Subscripts

i	PV panel type
j	Battery unit type
k	A time interval
s	WE stack type

Continuous Variables

H	Hydrogen pressure profile in storage tanks
P_{Bcj}	Power flow profile for charging battery j
P_{Bdj}	Power flow profile for discharging battery j
P_{BE}	Power flow profile from the battery bank to WE cluster
P_{BG}	Power flow profile from the battery bank to the local grid
P_{Es}	Power consumption profile of WE stack s
P_{GB}	Power flow profile from the local grid to battery bank
P_{GE}	Power flow profile from the local grid to WE cluster
P_{PB}	Power flow profile from solar PV farm to battery bank
P_{PE}	Power flow profile from solar PV farm to WE cluster
P_{PG}	Power flow profile from solar PV farm to the local grid
Q_{Bj}	Stored energy profile in the battery type j
R	Hydrogen production profile of WE cluster
t	Continuous time
X	Hydrogen inventory profile in cylindrical storage tanks
ρ	Hydrogen density profile in storage tanks

Integer Variables

M_s	Number of WE stacks of type s
N_i	Number of solar PV panels of type i
NC	Number of cylindrical storage tanks
U_j	Number of units of battery type j

Parameters

A^*	Maximum available land plot area (km^2) for building the facility
a_B	Annualization factor for battery bank
A^*_{Bj}	Area (m^2/unit) of battery j
a_E	Annualization factor for WE cluster
A_{Es}	Area (m^2/stack) of WE stack s
a_p	Annualization factor for solar PV farm
A_{Pi}	Area (m^2/panel) of PV panel i
C_{Bj}	Total installed cost ($/kWh) of battery j
C_{Es}	Total installed cost ($/kW) of stack s
C_L	Cost of land leasing ($/$km^2$)
C_{Pi}	Total installed cost ($/kW) of panel i
a_{ST}	Annualization factor for storage cylinders
C_{ST}	Total installed cost ($/cylinder) of storage cylinder
D	Hydrogen demand profile over time (tonne per hour)
D_{ST}	Diameter (m) of storage cylinder
EI	Emission intensity (tonne/kWh) for the grid power
$fopex$	Fixed annual operating cost fraction
H_{min}	Hydrogen delivery pressure (kPa) to the customers
H_{max}	Hydrogen delivery pressure (kPa) from the electrolyzers
H_0	Pressure in the storage tanks at time $t = 0$
I	Total types of PV panels
IR	Profile of solar irradiance (kW/m^2) over time
J	Total types of batteries
K	Total time intervals
L_{ST}	Length (m) of storage cylinder
P^*_{Bcj}	Power rating (kW/unit) for charging of battery j
P^*_{Bdj}	Power rating (kW/unit) for discharging of battery j
P_{IMP}	Limit on power purchase from the grid
P^*_{Es}	Power rating (kW/stack) of stack s
P_{EXP}	Limit on power sales to the grid
P^*_{Pi}	Rated capacity (kW/panel) of PV panel i
pb	Profile of electricity buying price ($/kWh) to grid
pc	Projected carbon tax ($/tonne)
ps	Profile of electricity selling price ($/kWh) to grid
Q^*_{Bj}	Storage capacity (kWh/unit) of battery j
R^*_{Es}	Hydrogen production rating (tonne per hour) of stack s
S	Total types of WE stacks
V	Volume of a cylindrical storage tank
α_i	Performance characteristics of solar PV panel type i
η_{cj}	Charging efficiency of battery j
η_{dj}	Discharging efficiency of battery j
η_{lj}	Dissipation efficiency of battery j
λ_B	Land footprint multiplier for battery
λ_E	Land footprint multiplier for water electrolyzer
λ_P	Land footprint multiplier for solar PV panels
λ_{ST}	Land footprint multiplier for storage cylinder
ρ_{min}	Density of hydrogen at H_{min} pressure in storage tanks
ρ_{max}	Density of hydrogen at H_{max} pressure in storage tanks
ρ_0	Density of hydrogen at H_0 pressure in the storage tanks

Symbols

$ACAPEX$	Annualized capital expenditure of the facility
$CAPEX$	Total capital expenditure of the facility

CTAX	Annual carbon tax payable	θ_A	Aggregate technology advancement factor
LCOH	Landed cost of hydrogen	θ_B	Battery technology advancement factor
LFP	Land footprint	θ_D	Discount rate advancement factor
REV	Net revenue from electricity sales to the grid	θ_E	WE technology advancement factor
T	Discrete time	θ_P	PV technology advancement factor
TAC	Total annualized cost		

phase, and with efficiencies ranging from 40 to 60%; hence, they may not factor into GH_2 production in the near term. Boretti [14] presented a commentary on various thermochemical routes for producing carbon free hydrogen powered by concentrated solar energy and estimated that these pathways may be competitive with electrolysis by 2030. On the other hand, biomass gasification to produce hydrogen is a commercially available technology. While it can play a key role, its large-scale usage is limited by biomass availability, the practically non-existent biomass supply chain, variable feedstock, and challenges for a continuous process. Hence, water electrolysis has received much of the attention in GH_2 production routes. Nikolaidis and Poullikkas [15] presented a comparative overview of fourteen different routes for hydrogen production. They highlighted that low efficiencies and high investment costs are the key hurdles for the water-splitting technologies to compete with the conventional methods.

The current status, research trends, and challenges in the water electrolysis technologies are discussed in detail in [16]. This work focused on the three most promising options, namely alkaline electrolysis (ALE), polymer electrolyte membrane (PEM), and solid oxide electrolysis (SOE) and discussed their electrochemical performances and limitations. It also presented possible solutions for improving the performances of these electrolyzers and highlighted the future directions in terms of cost and operational parameters. Among the three electrolyzer technologies, ALE is the most commercially advanced, and PEM and SOE are still in the early stages of development with low technology readiness level (TRL) [17]. The cost of hydrogen production via water electrolysis is expected to continually reduce over the coming decades with 66–85% reductions by 2050 [18]. Therefore, this work focuses on producing GH_2 via water electrolysis using solar energy. Furthermore, PEM and ALE technologies are considered for GH_2 production via water electrolysis due to their commercial availability. Despite its current low technology readiness level, PEM is included because it is advocated as more promising among the two emerging technology options. Henceforth, GH_2 will mean hydrogen produced from water electrolysis via renewable solar electricity.

The pace of GH_2 adoption will depend heavily on the economic competitiveness of its robust large-scale production. The produced hydrogen needs to be dried, purified, and suitably transformed for storage and transport or compressed and directly piped to the demand locations [19]. Currently, water electrolysis (WE) accounts for only 5% of global GH_2 production due to the cheaper black/grey/blue hydrogen from fossil fuels [11]. Hence, cost economics or LCOH (Landed Cost of H_2) is the key challenge facing GH_2 production. The literature is replete with studies on cost of production via different types of electrolyzers. Furthermore, there are works that focus on specific regions [20] or sectors [21]. Almost all of them restrict their analysis boundary around the water electrolysis plant (WEP). Nami et al. [22] presented a techno-economic analysis of water electrolysis for green hydrogen production wherein they considered two electrolyzer options, *viz.* ALE and SOE. Aspen Plus was used to simulate and analyze various WEP configurations, but the effect of intermittent renewable electricity was not considered. Furthermore, they assumed a constant renewable electricity cost and WEP capacity factor, which are often governed by the availability of renewable energy and provision of energy storage devices. Jang et al. [23] also assessed various WEP options through techno-economic analysis and their estimated LCOH was in the range of \$7–10/kg-H_2. Their analysis also relied on utilizing Aspen Plus for simulating various WEP configurations. Their technoeconomic analysis also assumed a fixed operational capacity factor for the WEP and fixed cost for renewable electricity. In another work, Jang et al. [24] considered the same scope with an addition of offshore wind power plant as a source of renewable energy. However, this work did not consider the impact of intermittent electricity generation by the wind power plant on the operation of the WEP. It mainly focused on assessing configurations for producing and transporting electricity vs. GH_2 from offshore locations to onshore demands. Manzotti et al. [25] evaluated the potential of membraneless electrolyzers for producing high purity and low cost GH_2 in China, the United States of America, Hong Kong, and the European Union. Biggins et al. [26] employed the Real Option method to assess the impact of dynamic power generation in a wind farm to operate the WEP. However, the options to operate WEP with battery storage, hydrogen storage, or sell-off of surplus electricity to the grid were not considered. Their main objective was to assess risk of investing in WEP now and to estimate the waiting period that averts the risk and enables financial gains. All these studies estimated the cost of GH_2 production; however, their scope was restricted to the water electrolysis plant only. The literature is replete with works [27] that focus on detailed analysis of electrolyzer performance and study electrochemical kinetics for various types of cells using modelling and simulation approaches. Additionally, the studies discussed so far did not consider the impact of the intermittent nature of renewable electricity generation. Rather, they assumed fixed availability and cost of renewable electricity, which can only be achieved through active energy management (*e.g.* energy storage devices) that comes at an additional cost. In essence, the literature has not considered an all-inclusive scope for the design and analysis of a GH_2 production facility.

Besides electrolysis technologies, the availability, intermittency, and dynamics of renewable solar energy influence LCOH. The intermittency and dynamics can be managed in two ways. One can size a WE plant to fully utilize the solar power instantaneously. In this route, the WE plant (WEP) must be sized for the highest irradiance level. It will operate mostly at part-load conditions during the day and shut down during the night, resulting in a low utilization *i.e.* a low operational capacity factor. The produced hydrogen must be stored to supply during the non-operational period; hence the additional cost of physical hydrogen storage is incurred. Alternately, one can install a battery storage system (BSS). This would enable the storage of the electrical energy produced during the day in excess of the WEP capacity and the stored energy will be used during the night. The utilization of WEP will increase and its size/capacity/cost will decrease, but additional cost of BSS will be incurred, and physical hydrogen storage may still be required. Clearly, balancing these multiple factors is not straightforward, as the truly optimal design may lie between the two extreme options. The problem becomes even more complex, when the dynamic variation in solar irradiance at a fine granularity in time is considered. The authors are aware of only two studies that have addressed the integration of BSS and WEP for GH_2 production. The Institute of Energy and Climate Research [28] showed that the addition of BSS increased solar-to-hydrogen efficiency despite battery losses. However, they did not address the cost economics. Another study [29] found a BSS to lower the economic performances of concentrated solar power plants and solar hydrogen plants due to the high cost of BSS. However, this conclusion was specific to retrofitting a pre-existing thermal-storage-based plant.

Clearly, it is critical to understand the relevance and impact of

various GH_2 production design decisions on LCOH to better guide future research advances and their real-life translation. To this end, the aim is to equip industry personnel and research community with a comprehensive and versatile model that can be employed to evaluate a variety of options for each of the technologies involved in the GH_2 production value chain and yield an optimal GH_2 production facility design. Note that, this is equivalent to pre-FEED (Front-End Engineering and Design) analysis, commonly performed in the industry. The GH_2 production facility model considers the local intensity profile of solar irradiance, physical hydrogen storage, land footprint, carbon intensity of the local grid, and various other factors (types, sizes, capital and operating costs, efficiencies, characteristics, lifespans) related to WE, battery storage, and solar PV (photovoltaic) technologies. Overall, the model bridges the gaps in the literature with following key novelties:

1. The analysis scope is expanded to consider the entire value chain of GH_2 production *i.e.* from renewable electricity generation, to its utilization and storage, to WEP operation, to hydrogen storage and dispensing.
2. The model accounts for the impact of intra-day and inter-day variations in renewable electricity generation by considering the solar irradiance data at a fine granularity.
3. The model enables an option to install batteries for storing and utilizing renewable electrons. Similarly, it also considers the storage of hydrogen molecules to manage hydrogen demand.
4. The model allows for an import from and export to the local electrical grid.
5. Lastly, the model can consider a variety of options for each technology (such solar PV, WE, battery storage) involved in the GH_2 facility and an optimal design with the least cost can be obtained.

Using this model, the work addresses a variety of questions, some of which are as follows:

1. How to select and size various technology components in a GH_2 production facility and design it with the least LCOH?
2. What is the minimum LCOH for a given technoeconomic and geographic landscape?
3. When should one install BSS and/or physical hydrogen storage?
4. Which WE technology may be good for GH_2 production?
5. How do the local power grid and its dynamic pricing impact the optimal design of a GH_2 production facility?
6. How does the optimal design of a GH_2 production facility vary with geographical location?
7. What are the relative contributions of various plant components to LCOH? Which advances will make the most impact on LCOH?

2. Mathematical model formulation

A facility producing green hydrogen from solar energy can have five main components as shown in Fig. 1.

1. A farm of PV panels for producing electricity from the sunlight,
2. A cluster of parallel WE stacks that use the above electricity to split water via electrolysis to produce hydrogen,
3. A bank of battery units for storing electrical energy temporarily,
4. Racks of horizontal cylindrical pressure vessels (buffer tanks) that receive hydrogen from the WE stacks (or simply stacks) and deliver it to the customers at a fixed supply pressure,
5. A pumping station that supplies water to the stacks.

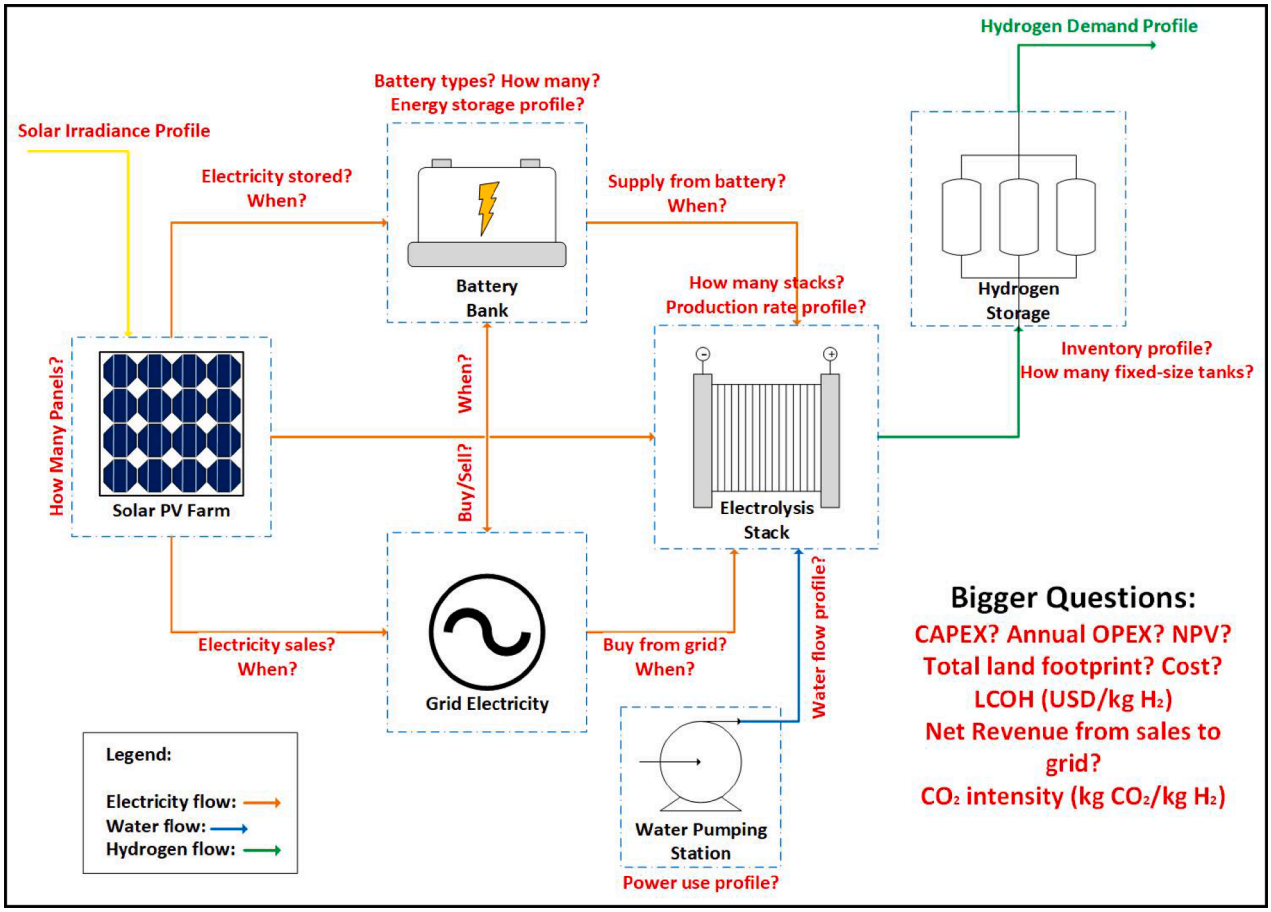

Fig. 1. A schematic for green hydrogen production facility with solar PV as the renewable electricity source.

The facility delivers H_2 gas to its customers at a fixed pressure. Here, the customers can be one or more industries (*e.g.* chemical production, steel manufacturing, etc.) and/or power plants near the hydrogen production facility. The facility is linked to a local power grid. It can sell power to or buy power from this grid at any time, for which the grid has published prices. The local grid may have CO_2 emissions. The main challenge in designing this facility is to use the transient and uncertain solar irradiance optimally to satisfy hydrogen demand at the least expense (*i.e.* minimum LCOH). Since the day-to-day operating costs (FOPEX) of the facility can be taken as a fraction of the total capital cost (CAPEX), the initial investment on various units (panels, stacks, batteries, buffer tank, and pump), revenue from electricity sales to the grid, expense for electricity purchase from the grid, and carbon tax paid for grid electricity purchase constitute the primary financial drivers. Appendix A presents a detailed problem statement along with all the assumptions.

With this, the goal is to develop a comprehensive model for a dedicated GH_2 production facility that caters to a given hydrogen demand. A GH_2 facility has five potential components, namely solar PV farm, WE plant cluster, battery bank, storage tank racks, and connectivity with the grid. Each of these components can be made up of multiple options based on available technology. For example, a solar farm can have several sub-plots, each with different types of solar panels. These five components are connected as follows. The electrical energy produced by solar PV farm can be supplied to WE cluster for hydrogen production, to battery bank for energy storage, and to the grid. Similarly, the local grid can also supply electricity to WE cluster for hydrogen production and to battery bank for energy storage. The stored energy from battery bank can be dispensed off to WE cluster as well as the local grid. Hydrogen produced in WE cluster is stored in tanks and these storage tanks cater to the known hydrogen demand. To this end, the mathematical model consists of energy balance equations for each component, energy flow balance equations across different connections, inventory balance equations on the storage tanks, and so on. With these constraints, TAC (total annualized cost) needs to be minimized to obtain the optimal facility design.

For the sake brevity and readability, the detailed model formulation with all the equations (Eqs. (1–17)) is presented in Appendix B. It is a mixed integer nonlinear programming (MINLP) problem, where number of WE stacks, number of solar panels, number of battery units, and number of storage tanks are discrete variables while all other variables are continuous. A numerical solution approach for solving the problem, subject to the assumptions is presented in Appendix C. The model is written and solved using GAMS (General Algebraic Modelling System), a well-known commercial software for mathematical optimization. BARON [30], a commercially available MINLP solver is used for solving the optimization problem.

The model is employed to obtain the optimal facility design that yields cheapest green hydrogen under different geographical and technoeconomic conditions. Furthermore, the potential impact of electricity trading between the GH_2 facility and the local grid on the cost of GH2, and its emission intensity is evaluated. Lastly, the model is utilized to understand the technoeconomic advancements needed in various components of the GH_2 facility and their contributions in making GH_2 cost-competitive with the current market price of hydrogen produced from hydrocarbon and biomass feed sources.

3. Case studies

The comprehensive mathematical model developed and solved in this study captures the crucial factors influencing the design of a GH_2 production facility and the associated LCOH. These include irradiance profiles that vary with geographical location, types of various plant components (*e.g.* stacks, batteries, …), their competitive technoeconomic features, and other constraints such as land footprint and grid power import/export. To understand the relative importance and impact of these factors on the design of a GH_2 facility, a fixed demand of 4.80 tonne per day (TPD) GH_2 is considered in four countries: KSA (Saudi Arabia), AUS (Australia), GER (Germany), and SIN (Singapore). This analysis assumes that two types of solar PV panels (SPV1 and SPV2), two types of WE stacks (PEM and ALE), and two types of battery units (BU1 and BU2) are available in the market. Table 1 lists the technoeconomic factors that differentiate these components and make them competitive. The irradiance data for one year (1st January 2020 to 31st December 2020) for these locations are obtained from NASA's public database [31]. The following four possible scenarios for this GH_2 production facility are considered.

Islanded Facility (ILF): A facility that is self-sufficient and fully isolated. It neither supplies to nor receives any electricity from any power grid. Such a facility has zero carbon emissions, so produces completely green hydrogen.

Facility with Grid Import (FGI): A facility that can import electricity from the local power grid but cannot sell any to the grid. Such a facility may not yield fully green hydrogen, as the grid may have a positive carbon intensity.

Facility with Grid Export (FGE): A facility that can export electricity to the local power grid but cannot import any electricity from the local grid. Such a facility will yield fully green hydrogen while reducing the burden on LCOH through additional revenue compared to ILF.

Facility with Grid Import and Export (FGIE): A facility that can both import electricity from and export electricity to the local power grid. Such a facility admits electricity price arbitrage in its operation and may have a positive carbon intensity.

Note that, all four nations are considered for analysis with ILF configuration while only Singapore is considered for analyses with FGE, FGI, and FGIE configurations because unlike the other three countries, the grid electricity prices at fine granularity are readily available for Singapore in the public domain.

3.1. Islanded facility (ILF)

An ILF must produce its GH_2 solely from the solar PV farm. Since it can produce GH_2 only during the day, storing GH_2 for the nighttime demand is critical. The present GH_2 facility can either store hydrogen physically in the cylindrical tanks or store electrons in the batteries. Hence, the facility deign involves a trade-off between battery storage and hydrogen storage. The impact on the size of the solar PV farm and number of WE stack will be minimal due to a small instantaneous self-discharge loss from the batteries. In order to show this trade-off, *NC* (total number of cylinders each with fixed volume) is varied and its impact on LCOH is observed. When *NC* is high, the plant should use no or minimal batteries, and vice versa. Fig. 1 shows LCOH versus *NC* for the four locations. LCOH drops with *NC* for all four locations and is the least for the no-battery scenario. This implies that storing hydrogen molecules is cheaper than storing electrons in the current technoeconomic landscape.

The minimum LCOH ($/kg-$H_2$) is 10.68 for KSA, 12.00 for AUS, 13.86 for SIN, and 42.12 for GER (see Table 2). The LCOH is relatively much higher for GER because of the seasonality and weakness of its solar irradiance. On the other hand, KSA has the lowest LCOH due to its strong and uniform solar irradiance throughout the year. These LCOH are estimated by assuming the cost of water to be zero. Nonetheless, as stated in Appendix B, fixed amount of water (9 kg) is required for producing 1 kg of hydrogen via electrolysis. Thus, given the cost of water across all locations, it is straightforward to compute LCOH inclusive of the local water cost. Currently, the commercial water prices are $0.002/kg in Saudi Arabia [32], $0.002/kg in Australia [33], $0.003/kg in Singapore [34], and $0.002/kg in Germany [35], thus the LCOH will increase by $0.018/kg-$H_2$ in Saudi Arabia (LCOH = $10.70/kg-$H_2$), $0.018/kg-$H_2$ in Australia (LCOH = $12.02/kg-$H_2$), $0.027/kg-$H_2$ in Singapore (LCOH = $13.89/kg-$H_2$), and $0.018/kg-$H_2$ in Germany (LCOH = $42.14/kg-$H_2$) after accounting for water cost.

Table 1
Technoeconomic parameters related to the various component options for the facility.

Parameter	Solar Panels		Electrolysis Stacks		Battery Units		Storage Cylinder
Label	SPV1	SPV2	PEM	ALE	BU1	BU2	SC
Rated Power,$\mathbf{P}_{\mathbf{E}}^{*}$ (kW/unit)	0.40	0.61	1138	2500	150	1000	NA
Rated Flowrate,$\mathbf{R}_{\mathbf{E}}^{*}$ TPH/stack	NA	NA	0.021	0.052	NA	NA	NA
Rated Capacity,$\mathbf{Q}_{\mathbf{B}}^{*}$ kWh/unit	NA	NA	NA	NA	230	2559	NA
Solar Panel Characteristic,α	0.30	0.46	NA	NA	NA	NA	NA
Efficiencies (η_c, η_d, η_l)	NA	NA	NA	NA	(0.95, 0.95. 0.05)	(0.95, 0.95. 0.05)	NA
Lifetime (y)	25	25	20	20	10	10	25
Area,**A** (m^2/unit)	2	2.77	70	70	2.80	15	8.53
Installed Cost,**C** ($/unit)	599	714	1.76E6	3.06E6	339	292	4.50E4
Area Multiplier,λ	2.50	2.50	2.50	2.50	1	1	0.50
Diameter,$\mathbf{D}_{\mathbf{ST}}$ (m)	NA	NA	NA	NA	NA	NA	1.17
Length,$\mathbf{L}_{\mathbf{ST}}$ (m)	NA	NA	NA	NA	NA	NA	7.29

$\mathbf{H}_{\mathbf{min}} = 2000$ kPa, $\mathbf{H}_{\mathbf{max}} = 3000$ kPa, $\rho_{\mathbf{min}} = 1.6$ kg/m^3, $\rho_{\mathbf{max}} = 2.4$ kg/m^3
fopex = 2%, Discount Rate = 8%, **CarbonTax** = \$50/**tonneCO**$_2$, $\mathbf{P}_{\mathbf{IMP}}^{*} = 2000$ kW, $\mathbf{P}_{\mathbf{EXP}}^{*} = 2000\mathbf{kWC}_{\mathbf{L}} = 0.10$ \$/m^2, $\mathbf{A}^{*} = 5$ km^2

Table 2
Summary of GH_2 production facilities yielding lowest LCOH across four countries based on Figs. 2-3.

Parameter	KSA	AUS	SIN	GER
LCOH ($/kg)	10.68	12.00	13.86	42.12
TAC (M$)	18.76	21.07	24.36	74.00
Total Installed Solar PV Capacity (kW)	75,626	80,828	101,026	419,692
SPV1 Panels	0	0	0	0
SPV2 Panels	123,977	132,505	165,616	688,019
Total Installed WE Plant Capacity (kW)	32,500	32,500	30,000	52,500
PEM Stacks	0	0	0	0
ALE Stacks	13	13	12	21
Gearing Ratio	2.33	2.49	3.37	7.99
Total Installed Battery Capacity (kWh)	0	0	0	0
BU1 Units	0	0	0	0
BU2 units	0	0	0	0
Hydrogen Storage Volume (m^3)	6586	9189	10,811	18,644
Cylinders	840	1172	1379	2378
Land Footprint (km^2)	0.86	0.92	1.15	4.78

When *NC* is low, the GH_2 facility cannot store hydrogen, thus its WE plant must produce hydrogen continuously at the demand rate. Therefore, in addition to a large solar PV farm, it also needs a large battery capacity, so that there is enough power to sustain its WE plant especially during the periods of weak irradiance (see Figs. 2 and 3). As the *NC* increases, the facility can produce and store surplus hydrogen during strong irradiance periods for use in weak/zero irradiance periods. In other words, the weakest solar irradiance period no longer governs the optimal facility design. This reduces the number of the solar panels and batteries but entails a larger WE plant capacity as shown in Figs. 2 and 3. In essence, the savings achieved with the smaller solar farm and battery storage capacity outweigh the cost increase in the WE plant and hydrogen storage in the current technoeconomic landscape at all locations. Clearly, the battery economics is still not competitive for GH_2 production despite the savings from increased WE stack utilization. The impacts of various technical advances on LCOH are discussed in the subsequent section.

Overall, the general trade-offs in designing a GH_2 facility emerge as follows. For a given storage capacity, one needs to obtain the optimal capacities of solar PV farm, battery storage, and WE plant. Since GH_2 demand is known and the facility is islanded, the size of solar PV farm is primarily governed by solar irradiance, *i.e.* geographical location. Furthermore, since day-to-day solar irradiance also varies at a given location, the period with the weakest irradiance also plays a role in determining solar PV farm size. Solar PV farm size decreases as the irradiance intensity increases. The battery capacity competes directly with hydrogen storage capacity. As the latter increases, the former decreases. At a given location, as the hydrogen storage capacity increases, the surplus production and storage of hydrogen during strong irradiance period becomes more viable. In other words, the energy that is being stored in batteries can now be instantly converted to hydrogen. By reducing battery storage capacity, the energy losses associated with batteries are also avoided, which further reduces solar PV farm slightly. Lastly, the WE plant can be sized to produce and store excess hydrogen during sunshine, which can be dispensed off during dark or low sunshine periods. Thus, the size of WE plant increases with hydrogen storage capacity. Clearly, so long the combined molecular storage and additional WE plant costs are more economical than electron storage, the optimal facility will not favor the use of battery storage.

Note that, the analyses so far fixed *NC* to obtain the optimal facility design. However, the truly optimal design will be the one in which *NC* is also a decision variable. The best facility designs thus obtained across the four locations are compared in Table 3. Interestingly, the LCOH for these designs are comparable with the ones for no-battery facilities (see Table 2), thus reinforcing the point about costly battery economics. The stronger the solar irradiance, the lower the LCOH and smaller the solar PV farm. For obvious reasons (*i.e.* seasonality and weakness of its solar irradiance), GER is the worst location for producing GH_2, as its LCOH is almost four times the LCOH at other locations. The four facilities can be compared based on their capacity gearing ratios, a ratio of solar PV capacity to WE capacity. The gearing ratios are 2.33 for KSA, 2.68 for AUS, 3.35 for SIN, and 9.97 for GER (Table 3). The smaller the gearing ratio, the better the location. In all cases, SPV2 panels prove to be more cost effective than SPV1. Only AUS installs a small number of SPV1 panels. ALE stacks are preferred over PEM, as they are cheaper. While KSA does not install any battery capacity, small battery capacities are installed in SIN and AUS. GER installs a significant battery capacity to reduce the burden on WE, however it comes at the expense of a larger solar PV farm compared to a no-battery scenario as there are losses

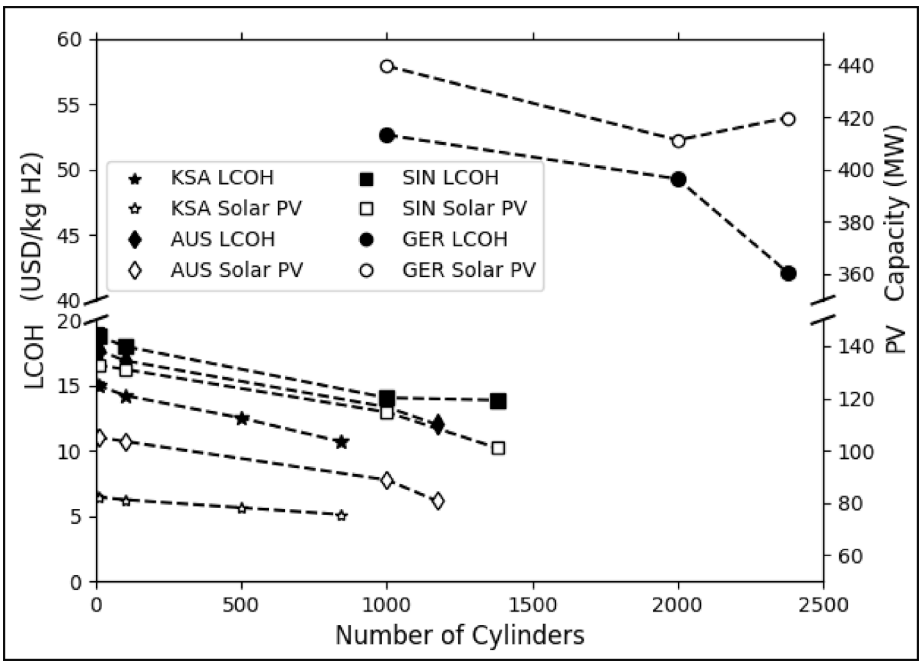

Fig. 2. Impact of storage cylinders on LCOH and Solar PV Farm capacity in Saudi Arabia, Australia, Singapore, and Germany.

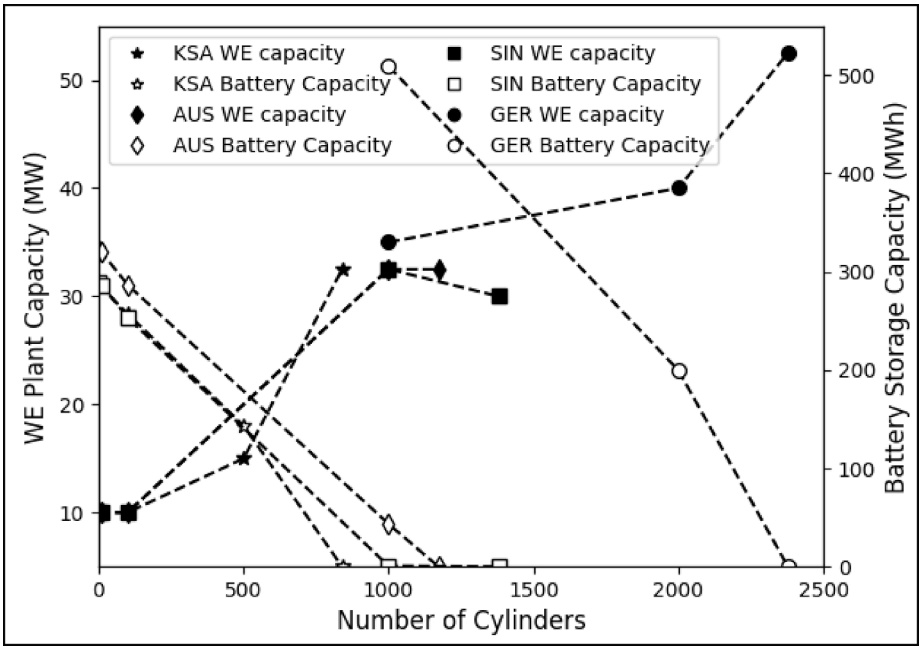

Fig. 3. Impact of storage cylinders on WE plant capacity and battery storage capacity in Saudi Arabia, Australia, Singapore, and Germany.

associated with battery storage. *NC* decreases, as intensity, stability, and duration of solar irradiance increases. For example, KSA has a longer duration of daily sunshine and lower seasonality, hence needs a lower *NC*. On the other hand, GER has a much higher seasonality and the larger variations in daily sunshine durations, thus needs a higher *NC*. Note that *NC* is governed by the duration of the worst irradiance period besides daily sundown periods.

Under the current technological landscape, GH_2 with LCOH of around 10+ \$/kg-H_2 is not competitive with grey/blue/orange hydrogen (with LCOH around 2–3+ \$/kg-H_2) [8]. Thus, it is useful to understand how technoeconomic advances in various GH_2 technologies as well as investment policies in green hydrogen (*e.g.* acceptance of lower return on investments) will lead to cost-competitive GH_2 production. This will pave the way for future research, development, and commercialization activities across various technology and policy verticals, *e.g.* cost reduction and life enhancement of batteries, need for low/no interest investments into GH_2 facilities (possibility of lower discount factors) etc. Before studying these, FGI, FGE, and FGIE are evaluated, which can reduce LCOH and show the impact of grid connectivity on LCOH.

3.2. Grid connected facilities

Now, the impact of grid connectivity on facility design, LCOH, and

Table 3
Summary of optimal GH_2 facilities for four countries.

Parameter	KSA	AUS	SIN	GER
LCOH ($/kg)	10.68	11.92	13.85	41.95
TAC (M$)	18.76	20.95	24.33	73.71
Total Installed Solar PV Capacity (kW)	75,626	80,323	100,412	423,813
SPV1 Panels	0	202	0	0
SPV2 Panels	123,977	131,545	164,610	694,775
Total Installed WE Plant Capacity (kW)	32,500	30,000	30,000	42,500
PEM Stacks	0	0	0	0
ALE Stacks	13	12	12	17
Gearing Ratio	2.33	2.68	3.35	9.97
Total Installed Battery Capacity (kWh)	0	6268	230	28,149
BU1 Units	0	5	1	0
BU2 units	0	2	0	11
Hydrogen Storage Volume (m^3)	6586	9157	10,874	17,452
Storage Cylinders	840	1168	1387	2226
Land Footprint (km^2)	0.86	0.92	1.15	4.82

carbon intensity is assessed. Since the study of FGI, FGE, and FGIE is for Singapore only, the discussion below is specific to Singapore.

LCOH ($/kg-$H_2$) for FGE, FGI, and FGIE in Singapore are 12.55, 11.78, and 10.44 respectively (Table 4). Clearly, grid connectivity in any configuration lowers LCOH compared to ILF (LCOH = $13.85 /kg-$H_2$). This is because FGE generates revenue by producing and exporting surplus solar electricity to the local grid, FGI reduces costs by exploiting the cheaper 24/7 grid power (average LCOE $0.17 /kWh vs $0.27 /kWh for battery), and FGIE does both. Hence, FGIE has the lowest LCOH. LCOH for FGI is lower than FGE because it is easier to import than export. The scope and reward for export are often more limited compared to import. In this case, grid export price is also much lower than GH_2 price, so the reward is limited. Interestingly, FGIE in SIN outperforms ILF in KSA (see Table 3), highlighting the power of grid-connected facilities. To enable power export, FGE uses 11% larger solar farm than ILF. In contrast, FGI uses 7% smaller solar farm, because it relies partially on the grid power. The 24/7 availability of grid power helps FGI to increase WE plant utilization and decrease WE plant capacity by 25% compared to ILF. Note that FGIE uses even smaller solar farm (9% smaller than ILF) than FGI. This clearly confirms that grid import outweighs grid export. The greater flexibility in FGIE enables greater capacity reductions. Even though these results are generated for GH_2 facility located in Singapore, the qualitative trends will be observed in other locations as well.

Although a grid-connected GH_2 facility yields lower LCOH, it cannot guarantee carbon-free hydrogen, until the grid achieves zero emission or carbon intensity (CI). Therefore, one cannot simply allow the use of grid electricity for GH_2 production, whenever renewable electricity is not available, which is often the case in the literature. Compared to the near-zero CI for GH_2, FGI hydrogen has a CI of 0.26 kg-CO_2/kg-H_2, and FGIE hydrogen has a CI of 0.31 kg-CO_2/kg-H_2. The carbon intensity of hydrogen is dependent on many factors including the emission factor of the grid electricity, limit on grid-imported electricity, carbon tax, etc. A larger grid emission factor yields a larger CI. Singapore's NG-based power sector results in grid emission factor of 0.41 kg-CO2/kWh that in turn yields CI of 0.26–0.31 kg-CO_2/kg-H_2. At the other extreme, locations with cheap coal-based power grid would result in even higher CI, thus highlighting that both price and carbon emissions should be considered while utilizing grid electricity.

Since grid connectivity lowers LCOH at the expense of increased CI, the focus should be on advances in solar PV, storage, and battery technologies. Therefore, the impacts of various technological advancements on LCOH and GH_2 facility design are analyzed next.

Table 4
Summary of optimal GH_2 facilities for three different grid-connected configurations in Singapore.

Parameter	FGI	FGE	FGIE
LCOH ($/kg)	11.78	12.55	10.44
TAC (M$)	20.70	22.05	18.34
LCOE from Solar Farm ($/kWh)	0.14	0.14	0.12
LCOE from Battery Storage ($/kWh)	0.27	0.24	0.25
CO_2 Footprint of Hydrogen (kg-CO_2/kg-H_2)	0.26	0	0.31
Total Installed Solar PV Capacity (kW)	93,061	111,516	92,829
SPV1 Panels	0	1	0
SPV2 Panels	152,559	182,813	152,179
Total Installed WE Plant Capacity (kW)	22,500	30,000	27,500
PEM Stacks	0	0	0
ALE Stacks	9	12	11
Total Installed Battery Capacity (kWh)	38,385	25,590	25,590
BU1 Units	0	0	0
BU2 units	15	10	10
Hydrogen Storage Volume (m^3)	5080	7495	4759
Storage Cylinders	648	956	607
Land Footprint (km^2)	1.06	1.27	1.06

4. Impact of technoeconomic advances

As discussed in Section 4, LCOH in the current technoeconomic landscape is not economically attractive. However, several factors such as solar PV cost, WE cost, battery cost, low-interest incentives, government subsidies, etc. can also affect LCOH, and their relative impacts are worth studying. To this end, the versatile model can help researchers and/or industry decision-makers to steer efforts towards key technological advancements. Therefore, the sensitivity of LCOH is conducted with respect to four factors, namely CAPEX of PV technology (*PVT*), CAPEX & rated yield of WE technology (*WET*), CAPEX of battery technology (*BST*), and discount factor (*DF*). Consider two options each for solar panels (SPV1 and SPV2), WE stacks (PEM and AEL), and batteries (BU1 and BU2) as shown in Table 1. Since a facility with the least storage ($NC = 1$) demanded the largest battery capacity and highest LCOH (see Table 2), $NC = 1$ is fixed for assessing the impact of various technological advances (especially battery storage technology) on LCOH. Moreover, ILF configuration is used for the analysis to isolate benefits of technological advances. Note that, this analysis is limited to KSA, AUS, and SIN because even with technological advances GER cannot compete with other countries due to its seasonality and weaker irradiance.

The goal is to draw a holistic picture of technoeconomic evolution and its impact on LCOH in KSA, AUS, and SIN. For this, relative technoeconomic states of GH_2 facility and its components are defined as follows. Let θ_P, θ_E, θ_B, and θ_D denote the state of *PVT*, *WET*, *BST*, and *DF* respectively, with $\theta_P = 1$, $\theta_E = 1$, $\theta_B = 1$, and $\theta_D = 1$ representing the current technoeconomic landscape. Then, an aggregate technology advancement factor (*ATAF*) is defined as $\theta_A = \theta_P \times \theta_E \times \theta_B \times \theta_D$. Thus, $\theta_A = 1$ for the current technoeconomic landscape. As the technologies mature, θ s reduce. For example, if an advance in PV technology reduces its CAPEX by 10%, then $\theta_P = 0.90$, and so on. To this end, the impact of one technoeconomic factor at a time is assessed while keeping other technoeconomic factors at their current state. For example, when assessing the advancements in solar PV CAPEX factor, only θ_P is varied while fixing $\theta_E = 1$, $\theta_B = 1$, $\theta_D = 1$. Later, this approach is extended by performing one factor at a time analysis while fixing the other technoeconomic factors at some evolved state *i.e.*, $\theta \leq 1$. Note that these analyses are performed and discussed for KSA, AUS, and SIN.

Although solar PV technology has evolved significantly over the last two decades, further cost reductions are still possible. Hence, first consider 20% ($\theta_P = 0.80$), 40% ($\theta_P = 0.60$), and 60% ($\theta_P = 0.40$) reductions in solar PV CAPEX. With all other technologies at their current states ($\theta_E = 1$, $\theta_B = 1$, and $\theta_D = 1$), it is observed that LCOH drops consistently with reducing solar PV CAPEX for KSA, AUS, and SIN as shown in Figs. 4-6, respectively. KSA still offers the least LCOH of $10.14 / kg-$H_2$. Interestingly, LCOH in SIN becomes competitive with AUS, and ultimately surpasses AUS at 60% reduction ($13.09 /kg-$H_2$ in AUS versus $13.00 /kg-$H_2$ in SIN). This highlights that the reduction in solar

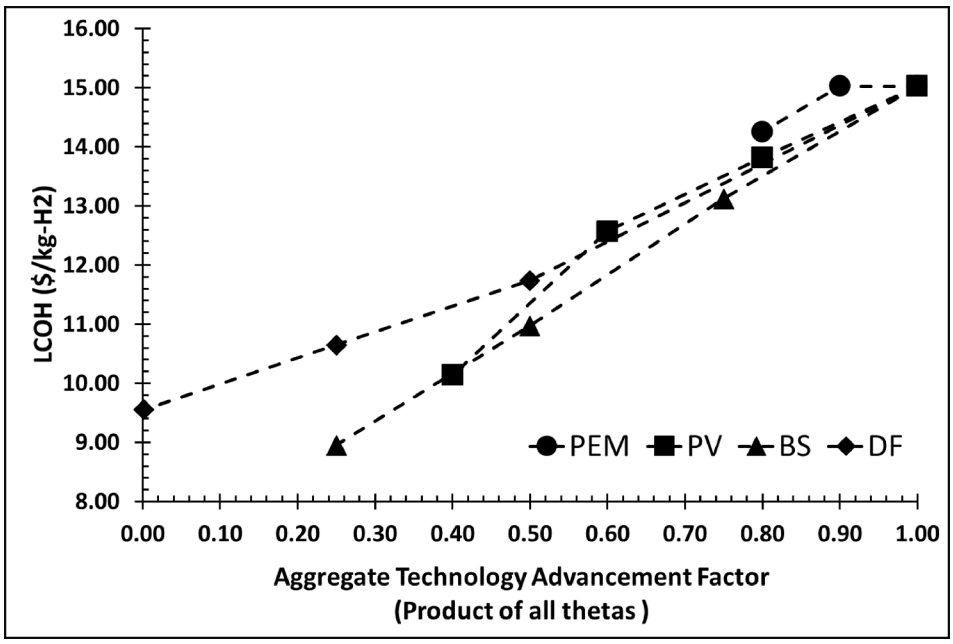

Fig. 4. Effect of advancements in technoeconomic factors of PV, BS, PEM, and DF on LCOH in KSA. θ_P, θ_B, θ_E, and θ_D denote technological states of PV, BS, PEM, and DF respectively. Only one technological state varies at a time while others remain at their current state *i.e.* at value of 1. The legend gives the technological state that is changed.

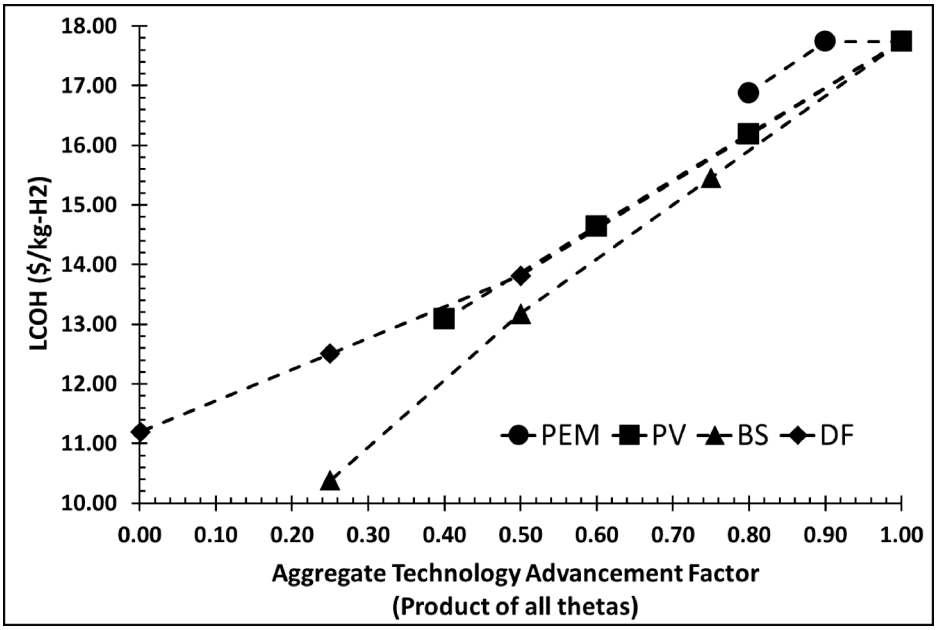

Fig. 5. Effect of improvements in techno-economic factors of PV, BS, PEM, and DF on LCOH in AUS. θ_P, θ_B, θ_E, and θ_D denote technological states of PV, BS, PEM, and DF respectively. Only one technological state varies at a time while others remain at their current state *i.e.* at value of 1.

PV CAPEX can help GH_2 in locations with relatively weaker, but uniform solar irradiance. Overall, LCOH reduces by \$0.60-\$0.98 /kg-H_2 for every 10% reduction in solar PV CAPEX.

Currently, PEM electrolyzer is at a relatively lower TRL than AEL. Thus, AEL electrolyzers are normally preferred over PEM due to better costs and yields. It is natural to ask what improvements may make PEM technology outperform AEL. To this end, consider 10% ($\theta_E = 0.90$) and 20% ($\theta_E = 0.80$) advances in PEM. It is observed that a 10% increase in rated yield and 10% decrease in CAPEX ($\theta_E = 0.90$) do not reduce LCOH at any location (see Figs. 4-6). In other words, PEM is not competitive with ALE with only 10% improvement (see Table 5). However, with a 20% improvement ($\theta_E = 0.80$), PEM becomes more economical than ALE at all locations. Note that PEM needs more stacks than ALE (Table 5), because its rated power is lower. LCOH reduces to \$14.26 /kg-H2 from \$15.03 /kg-H2 in KSA, to \$16.88 /kg-H2 from \$17.74 /kg-H2 in AUS, and to \$17.90 /kg-H2 from \$18.85 /kg-H2 in SIN. The reductions are below \$1/kg-H2 at all locations. This implies that significant cost benefit is unlikely without a major breakthrough in electrolyzer technologies.

Recall that the battery technology did not seem economical in the current technoeconomic landscape. Several ongoing efforts promise reductions in battery costs over the next two decades [36], which would

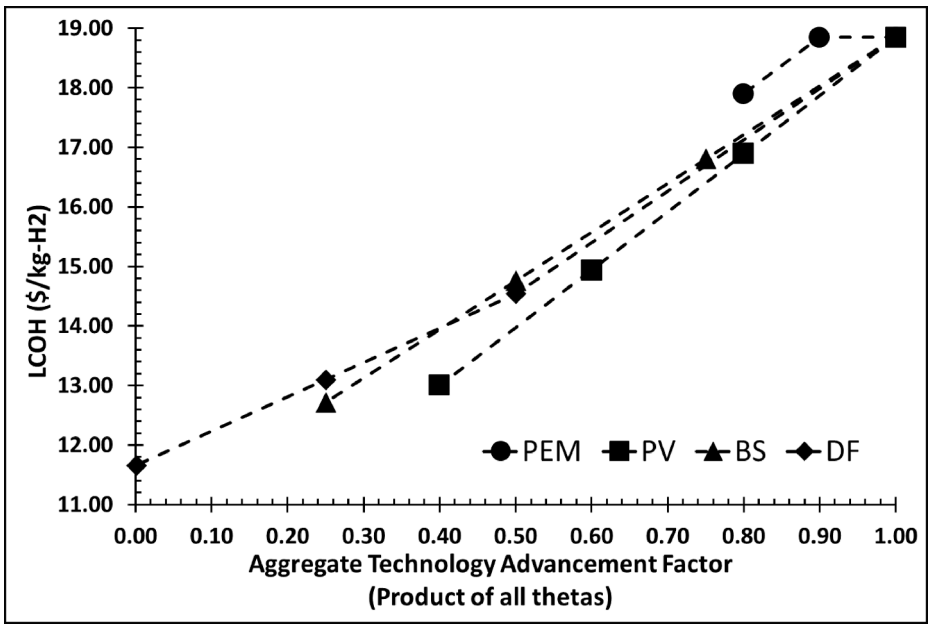

Fig. 6. Effect of improvements in techno-economic factors of PV, BS, PEM, and DF on LCOH in SIN. θ_P, θ_B, θ_E, and θ_D denote technological states of PV, BS, PEM, and DF respectively. Only one technological state varies at a time while others remain at their current state *i.e.* at value of 1.

Table 5
ALE and PEM stacks under various PEM technological advances.

Technological Advance in PEM (%)	PEM Stacks			ALE Stacks		
	KSA	AUS	SIN	KSA	AUS	SIN
0	0	0	0	**4**	**4**	**4**
10	0	0	0	**4**	**4**	**4**
20	**8**	**9**	**9**	0	0	0

decrease their CAPEX. Therefore, consider 25% ($\theta_B = 0.75$), 50% ($\theta_B = 0.50$), and 75% ($\theta_B = 0.25$) reductions in battery CAPEX. The assessment reveals that LCOH reduces by \$0.76–0.98 /kg-H_2 for every 10% reduction in battery CAPEX in all three locations. All three locations exhibit similar trends with the least LCOH at KSA (\$9.95 /kg-H_2) followed by AUS (\$10.38 /kg-H_2) and SIN (\$12.72 /kg-H_2), as shown in Figs. 4-6 respectively. Clearly, even with 75% reduction in battery CAPEX, LCOH reduces by 33%-42% only, and does not make GH_2 competitive against blue/orange H_2 (LCOH = \$2–3 /kg-H_2).

Thus far, the impact of various technological advancement on the LCOH is assessed and there is no top contender that would result in a large reduction in LCOH. Thus, it poses the question whether changes in financial policies could help reduce LCOH. So far, all the financial analyses assumed a standard discount factor of 8%. The discount factor is often set based on investor expectations and reflects expected returns on the entire investment into the project. Of course, the higher the discount factor, the higher the expected return on the investments, which consequently results in higher LCOH. Thus, reduction in the discount factor can yield lower LCOH. Such lowering of discount factor is possible through green sector investment at low interest rates, interest-free loans by governments, etc. To this end, consider three discount factors: 4% ($\theta_D = 0.50$), 2% ($\theta_D = 0.25$), and 0.01% ($\theta_D = 0.00125$). Note that discount factor of 0.01% represents practically zero return on the investment. While LCOH drops sharply when discount factor reduces from 8% to 4% in all locations, the drop becomes shallower when discount factor reduces from 4% to 0.01%. This is attributed to the nonlinear relationship between thse annualization factor and the discount factor. Even with 0.01% discount factor, the least LCOH of \$9.55/kg-H_2 is obtained in KSA followed by \$11.20/kg-H_2 in AUS, and \$11.66/kg-H_2 in SIN under the current technoeconomic landscape. Overall, the LCOH decreases by ~\$0.7–1.1/kg-H_2 for every percent drop in the discount factor.

Clearly, the low/no interest investments alone will not yield cost competitive GH_2 under the current technoeconomic landscape. The technologies involved in GH_2 facility, especially solar PV and battery storage need to evolve rapidly and simultaneously to allow for economical GH_2 production. The technological advancements combined with government subsidies and/or green investment schemes would yield cost competitive GH_2. To this end, a sequential evolution of technologies (WE, PV, and BS) is performed followed by financial subsidies (DF) to understand the least possible LCOH. In other words, first starting at a node ($\theta_P, \theta_E, \theta_B, \theta_D$) denoting the current technoeconomic state *i.e.* (1.00, 1.00, 1.00, 1.00) and θ_E is reduced from 1.00 to 0.80 while keeping θ_P, θ_B, and θ_D at 1 (see Figs. 7-9 for KSA, AUS, and SIN respectively). Next, starting at a node (1.00, 0.80, 1.00, 1.00), θ_P is reduced systematically to 0.40. Subsequently, the same approach is used to draw branches by reducing θ_B starting at (0.40, 0.80, 1.00, 1.00), reducing θ_D starting at (0.40, 0.80, 0.25, 1.00), reducing θ_B starting at (0.60, 0.80, 1.00, 1.00), and reducing θ_D starting at (0.60, 0.80, 0.50, 1.00). Such an approach enables us to paint a comprehensive picture of evolution of LCOH with advancements in various technoeconomic factors.

One can easily look at LCOH given the advances in PV, PEM, BS, and DF factors. For example, an LCOH of \$3.70/kg-H_2 is obtained in KSA (Fig. 7), \$4.34/kg-H_2 in AUS (Fig. 8), and \$4.69/kg-H_2 in SIN (Fig. 9) for a facility with no hydrogen storage when solar PV CAPEX is reduced by 60%, WE CAPEX is reduced by 20%, battery CAPEX is reduced by 75%, and the discount factor is only 2%. Similarly, one can choose to start at any node and change any of the factors to understand its impact on LCOH with respect to various combinations of advances in the other factors. Overall, these analyses highlight that though GH_2 has a potential to be a carbon-free energy source, significant advances across various associated technology frontiers and policy initiatives are required for the green hydrogen to become a reality.

5. Conclusions

This work developed and solved a rigorous, comprehensive, and versatile optimization model for designing a GH_2 production facility to

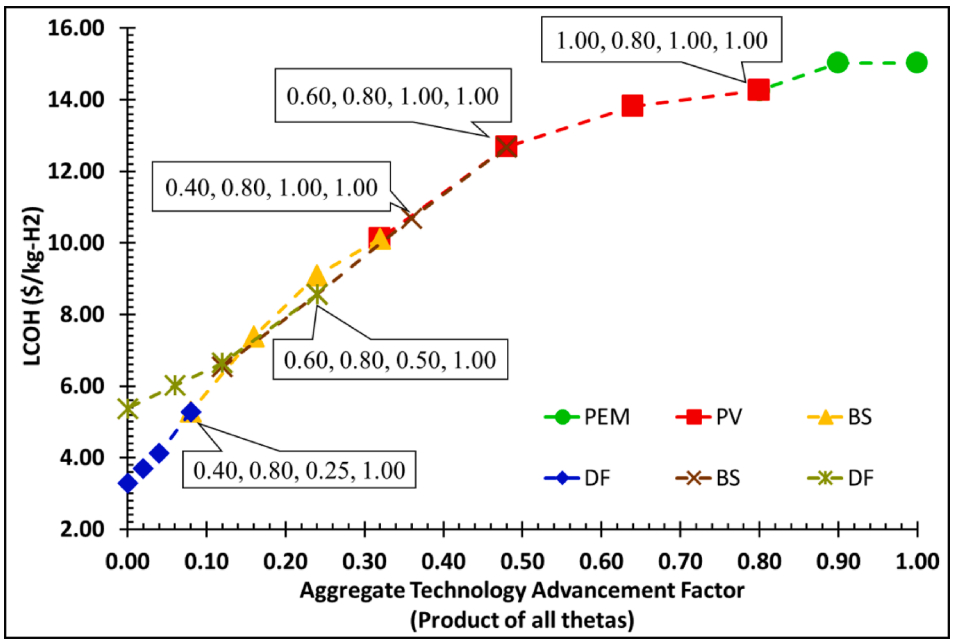

Fig. 7. Impact of technoeconomic evolution on LCOH in KSA. θ_P, θ_B, θ_E, and θ_D denote technological states of PV, BS, PEM, and DF respectively. Each branch starts at a node and the numbers at each node are θ values for PV, PEM, BS, and DF respectively. The legend gives the technological state that is changed and the starting node values of each branch are given in the following order θ_P, θ_B, θ_E, θ_D.

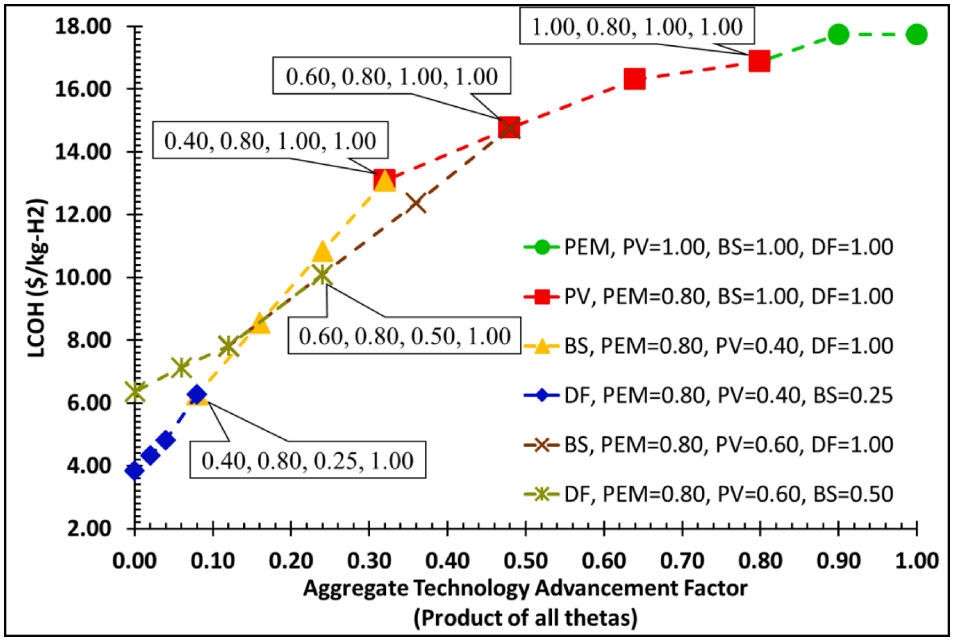

Fig. 8. Impact of technoeconomic evolution on LCOH in AUS. θ_P, θ_B, θ_E, and θ_D denote technological states of PV, BS, PEM, and DF respectively. Each branch starts at a node and the numbers at each node are θ values for PV, PEM, BS, and DF respectively. The legend gives the technological state that is changed and starting node of each branch is shown in order θ_P, θ_B, θ_E, θ_D.

achieve the least LCOH/TAC. The model accommodates several technoeconomically competitive options for solar PV panels, battery storage units, and WE stack. It also allows electricity import from and export to the local grid. More importantly, it accounts for both intra-day and day-to-day variations in solar irradiance essential for an optimal facility design.

The impact of availability and intensity of solar irradiance on the GH_2 facility design and LCOH is evident from the analyses across four locations. Saudi Arabia offers the cheapest GH_2 while Germany offers the costliest. Even though Saudi Arabia and Australia are seen as prominent candidates for GH_2 production, the former outperforms the latter by 10% in terms of LCOH under the current technoeconomics. Germany suffers from harsh seasonal conditions resulting in large variations in solar intensity and availability, thereby yielding the highest LCOH. The islanded GH_2 facility needs to store electrons in batteries or hydrogen molecule in storage tanks to ensure that the given GH_2 demand is met irrespective of sunshine availability. In the current technoeconomic landscape, the hydrogen molecule storage in tanks appears to be cheaper than electron storage in batteries. Therefore, the optimal GH_2 facilities in all locations had negligible battery capacity except

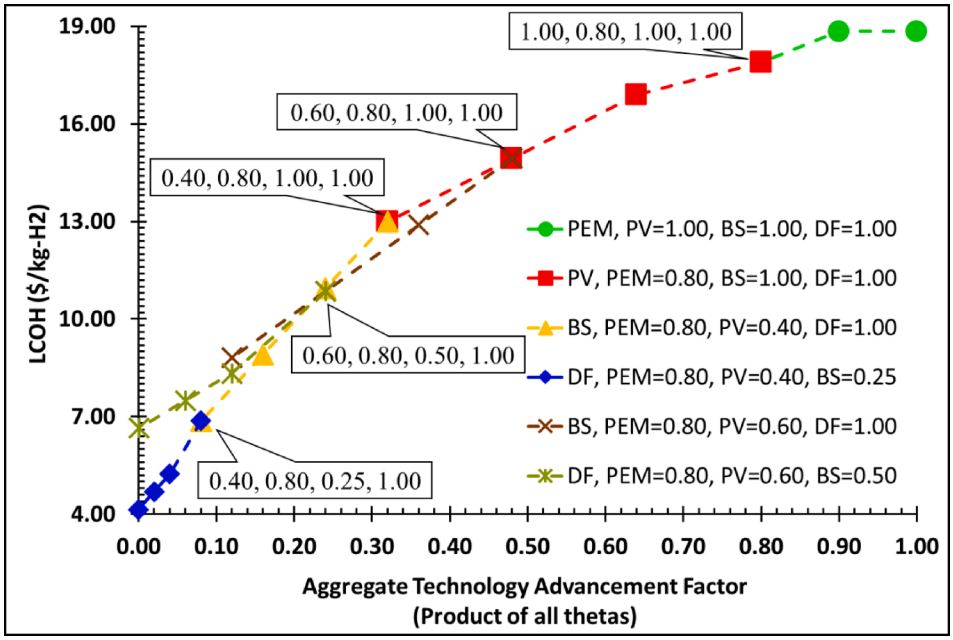

Fig. 9. Impact of technoeconomic evolution on LCOH in SIN. θ_P, θ_B, θ_E, and θ_D denote technological states of PV, BS, PEM, and DF respectively. Each branch starts at a node and the numbers at each node are θ values for PV, PEM, BS, and DF respectively. The legend gives the technological state that is changed and starting node of each branch is shown in order θ_P, θ_B, θ_E, θ_D.

Germany. This also highlights that the battery technology needs to rapidly advance to compete with tank storage. Interestingly, the installed hydrogen storage capacity is dictated by the worst sunshine period experienced by GH_2 facility. The stabler and more uniform the solar irradiance, the lower the hydrogen storage capacity.

Connectivity with the local grid offers opportunities to import cheap electricity to the GH_2 facility (FGI and FGIE) and to generate revenue by exporting electricity to the grid (FGE and FGIE). Irrespective of the configurations, the grid connectivity helps reduce LCOH compared to the islanded facility. Availability of often cheaper and around-the-clock grid electricity in FGI and FGIE not only reduces installed capacity of solar PV farm but also increases the utilization rate, and in turn reduces the installed capacity of the WE plant. FGE, on the other hand, installs larger solar PV capacity (compared to islanded facility) to exploit revenue from the sale of surplus electricity. Despite the economic benefits, hydrogen produced in a facility with an option to import from the grid (FGI and FGIE) has a positive carbon intensity (CI) unless the grid electricity is also green. Therefore, only FGE can guarantee zero-emissions hydrogen. The magnitude of CI in a facility with an option to import from the grid depends on the emission factor of the grid among other things. Thus, it is crucial to account for grid emissions when designing a GH_2 facility with grid connectivity, which is often ignored in practice.

Although the current technoeconomic landscape does not yield cost competitive GH_2, the technologies behind components involved in GH_2 production are advancing rapidly. Such advancements are conducive for lowering LCOH, thus opening the prospect of making GH_2 economically viable. Improvements in WE technology can help reduce LCOH to some extent, however, deep reduction in solar PV and battery storage CAPEX are needed to yield cheaper GH_2. With cheaper solar PV panels, the locations with uniform but weaker solar irradiance can also produce cheaper GH_2. Furthermore, if the solar electricity becomes extremely cheap, then the WE CAPEX factor would govern the LCOH. Besides technological advancements, low-interest loans/investments are also required to make GH_2 economically competitive with grey/blue/orange hydrogen. Overall, this comprehensive analysis offers an approach to draw a holistic picture of how LCOH evolves over different technological progress and financial incentive trajectories. Ultimately, LCOH ($ /kg-H_2) of 3.29 to 4.15 can be achieved with 60% reduction in solar PV CAPEX, 20% advancement in WE, 75% reduction in battery CAPEX, and discount factor of 0.01%.

Even though GH_2 has the potential to be a carbon-free energy source, rapid advancement across various technologies as well as investment policies are needed before green hydrogen can economically compete with the other low carbon options derived from the traditional energy vectors. Indeed, GH_2 seems like a potential yet costly silver bullet for deep decarbonization at this time.

CRediT authorship contribution statement

Sushant S. Garud: Conceptualization, Methodology, Software, Formal analysis, Writing – original draft. **Fanlok Tsang:** Resources, Visualization. **Iftekhar A. Karimi:** Conceptualization, Writing – review & editing, Project administration, Funding acquisition. **Shamsuzzaman Farooq:** Conceptualization, Writing – review & editing, Funding acquisition.

Declaration of Competing Interest

The authors declare the following financial interests/personal relationships which may be considered as potential competing interests: Dr. Sushant Garud reports financial support was provided by Exxon-Mobil Research and Engineering Company.

Data availability

Data will be made available on request.

Acknowledgement

Financial support from ExxonMobil through the Singapore Energy Center, under Grant LAW-2019-3484 (EM11161. TO5) is gratefully acknowledged. The authors are also thankful to Dr Bryan Chapman, Dr Robert Johnson, and Dr Adam Usadi from Exxon Mobil Research and Engineering for discussions and suggestions.

Appendix A:. Production facility design problem

The hydrogen facility delivers H_2 gas to its customers at a fixed pressure (H_{min} kPa). Here, the customers can be one or more industries (*e.g.* chemical production, steel manufacturing, etc.) and/or power plants near the hydrogen production facility. All stacks, irrespective of their cathode pressures, deliver hydrogen at a fixed pressure (H_{max} kPa). In other words, ALE with cathodes at 1 bar have in-built compressors to deliver hydrogen at H_{max} kPa. Given these fixed inlet and outlet pressures, hydrogen in the storage cylinders remains within $[H_{min}, H_{max}]$ kPa.

The facility is linked to a local power grid. It can sell power to or buy power from this grid at any time, for which the grid has published prices. The local grid may have CO_2 emissions. The main challenge in designing this facility is to use the transient and uncertain solar irradiance optimally to satisfy hydrogen demand at the least expense *(i.e.* minimum LCOH). Since the day-to-day operating costs (FOPEX) of the facility can be taken as a fraction of the total capital cost (CAPEX), the initial investment on various units (panels, stacks, batteries, buffer tank, and pump), revenue from electricity sales to the grid, expense for electricity purchase from the grid, and carbon tax paid for grid electricity purchase constitute the primary financial drivers.

In this work, such a facility is designed from grassroots. Given the sun's natural annual cycle, one year of operation forms the basis for the design. The design problem can be stated as follows:

Given:

1. Hydrogen demand profile ($D(t)$ tonne/h or tph) for a year,
2. Hydrogen supply pressure (H_{min} kPa),
3. I PV-panel types/sizes ($i = 1, 2, \cdots, I$) with rated capacities (P^*_{Pi} kW/panel), irradiance receiving areas (A_{Pi} m^2/panel), and total installed costs (C_{Pi} \$/kW),
4. S WE-stack types ($s = 1, 2, \cdots, S$) with power ratings (P^*_{Es} kW/stack), maximum operating pressure ($H_{max,s}$ kPa), hydrogen production ratings (R^*_{Es} tph), land footprints (A_{Es} m^2/stack), and installed costs (C_{Es} \$/kW),
5. J battery types ($j = 1, 2, \cdots, J$) with storage capacities (Q^*_{Bj} kWh/unit) and power ratings (P^*_{Bj} kW), charging, discharging, and dissipation characteristics ($\eta_{cj}, \eta_{dj}, and \eta_{lj}$), footprints ($A_{Bj}$ m^2), and total installed costs (C_{Bj} \$/kWh),
6. Length (L_{ST} m) and internal diameter (D_{ST} m) of the horizontal cylindrical buffer tanks, and the tank's total installed cost (C_{ST}\$/cylinder),
7. Land footprint (*LFP*) multipliers (λ_P, λ_B, λ_E, and λ_{ST}) for the land areas required by the installed PV panels, batteries, stacks, and buffer tank respectively,
8. Projected selling price ($ps(t)$ \$/kWh) and limit ($P_{EXP}(t)$ kW) on power sales to the grid,
9. Projected buying price ($pb(t)$ \$/kWh) and limit ($P_{IMP}(t)$ kW) on power purchase from the grid,
10. Projected carbon tax ($pc(t)$\$/tonne) and emission intensity (*EI* tonne/kWh) for the grid power,
11. Detailed solar irradiance ($IR(t)$ kW/m^2) profile for a year,
12. Maximum available land plot area for the facility (A^* km^2), and cost (C_L\$/km^2) of leasing,
13. Fixed annual operating cost as a fraction (*fopex*) of the total capital investment.

Determine:

1. Number (N_i) of PV panels of type $i = 1, 2, .., I$;
2. Number (M_s) of WE stacks of type $s = 1, 2, \cdots, S$;
3. Number (*NC*) of the cylindrical storage tanks,
4. Number (U_j) of units of battery type $j = 1, 2, \cdots, J$;
5. Hydrogen production rate of the facility versus time for the year,
6. Solar power generation (kW) versus time for the year,
7. Power sold (kW) to the grid versus time for the year,
8. Power purchased (kW) from the grid versus time for the year,
9. Energy storage (kWh) in the battery bank versus time for the year,
10. Hydrogen inventory (tonne) in the buffer tanks versus time for the year,
11. Total land footprint of the entire facility (km^2),
12. LCOH (\$/kg-H_2),
13. Carbon emissions (kg CO_2 per kg H_2) for producing GH_2.

Minimizing:

Net annual expense (\$/y) for the entire facility or equivalently LCOH.

Assuming:

1. The entire facility is isothermal. This assumption is made to simplify the effects of temperature on the performance various components (such as electrolyzers, batteries, etc.) involved in the facility.
2. All panels and stacks of a given type are identical.
3. Solar power from the PV panels can be controlled dynamically and automatically by turning the panels on/off to match the power intake by the facility.
4. The anodes of all stacks are at 1 bar, so the pumping station does not need much power to supply water to the stacks.

5. All stacks deliver hydrogen at H_{max}. In other words, the cathodes in all stacks are at H_{max}. If a cathode is not at H_{max}, then a compressor exists inside the stack to pressurize the released hydrogen to H_{max}. The cost and power rating of the compressor are absorbed in the stack parameters. Overall, any stacks irrespective of their types, supply hydrogen at H_{max}.
6. The input power to a stack of type/size cannot exceed P^*_{Es}.
7. Production rate of a stack varies linearly with input power.
8. Power generated by the PV panel varies linearly with the incident irradiance.
9. M_s stacks always operate at an identical rate.
10. Batteries can charge and discharge at the same time.
11. Instantaneous self-discharge rate (kW) of a battery is a fraction of its energy content.
12. No power losses for transfers among the solar farm, local grid, battery bank, and stack cluster.
13. Costs of water, water pump, and pumping energy are zero.
14. Inventory of hydrogen in the buffer tank varies linearly with its pressure.

Appendix B:. Mathematical model

With no loss of generality, the analysis year starts at the sunset of an arbitrary Dec 31, and ends at the sunset of the next Dec 31. If *t hour* denotes time (h), then $t = T_0 = 0$ (h) at the sunset of the starting Dec 31, and $t = T_K = T$ (h) at the sunset of the ending Dec 31. Henceforth, subscript P is used to denote the PV farm, B to denote the battery bank, G to denote the local grid, E to denote the stack cluster, W to denote the water pump, and NC to denote the buffer tanks for hydrogen storage.

The PV farm can host at most I subplots ($i = 1,2,\cdots,I$), each with N_i identical panels of type/size i. Each subplot i can generate at most $\alpha_i N_i IR(t)$ kW of power at time t, where $IR(0 \le t \le T)$ kW/m^2 is the incident solar irradiance and α_i m^2/panel captures performance characteristics such as efficiency, rated generation capacity, and receiving area for panel-type i, and the earth's standard irradiance. Clearly, $IR(t) = 0$, when there is no sunlight. The PV farm can supply this power to three entities:$P_{PE}(t)$ kW to the WE cluster, $P_{PB}(t)$ kW to the battery bank, and $P_{PG}(t)$ kW to the local grid. Then, a power balance on the PV farm gives us,

$$\sum\nolimits_{i=1}^{I} \alpha_i N_i IR(t) \ge P_{PE}(t) + P_{PB}(t) + P_{PG}(t) \quad 0 \le t \le T \tag{1}$$

The WE cluster can have at most S sub-plants, each with M_s stacks of type/size s. Each sub-plant s can consume $M_s P^*_{Es}$ kW of power. At time t, the WE cluster can receive power from three sources: $P_{PE}(t)$ kW from the PV farm, $P_{BE}(t)$ kW from the battery bank, and $P_{GE}(t)$ kW from the local grid. The total power from these sources must exceed that consumed by the S WE sub-plants.

$$P_{PE}(t) + P_{GE}(t) + P_{BE}(t) \ge \sum\nolimits_{s=1}^{S} P_{Es}(t) \quad 0 \le t \le T \tag{2a}$$

where, $P_{Es}(t)(0 \le t \le T, s = 1,2,\cdots,S)$ is the power consumed by sub-plant s at time t. This power must be less than its rated capacity as the model assumes that the stacks cannot consume more than rated capacity.

$$P_{Es}(t) \le M_s P^*_{Es} \quad 0 \le t \le T, \;\; 1 \le s \le S \tag{2b}$$

Therefore, the WE cluster produces $R(t)$ tph of hydrogen at time t.

$$R(t) = \sum\nolimits_{s=1}^{S} \frac{R^*_{Es}}{P^*_{Es}} P_{Es}(t) \quad 0 \le t \le T \tag{3}$$

If $D(t)$ tph is the demand rate at time t, then the inventory $X(t)$ tonne of hydrogen in the buffer tanks is given by,

$$\frac{dX(t)}{dt} = R(t) - D(t) \quad 0 \le t \le T \tag{4a}$$

$$X(0) = X(T) = NC \bullet V\rho_0 \tag{4b}$$

$$NC \bullet V\rho_{min} \le X(t) \le NC \bullet V\rho_{max} \quad 0 \le t \le T \tag{4c}$$

where, V m^3 is the volume of one cylindrical tank, NC is the number of tanks, ρ_{min} tonne/m^3 is the density of hydrogen at H_{min}, ρ_0 tonne/m^3 is the density of hydrogen at the buffer pressure (H_0 kPa) at time zero, ρ_{max} tonne/m^3 is the density of hydrogen at H_{max}. Instead of $X(t)$, hydrogen density [$\rho(t)$ tonne/m^3] in the tanks can be used to measure its inventory.

$$NC \bullet V\frac{d\rho(t)}{dt} = R(t) - D(t) \quad 0 \le t \le T \tag{5a}$$

$$\rho(0) = \rho(T) = \rho_0 \tag{5b}$$

$$\rho_{min} \le \rho(t) \le \rho_{max} \quad 0 \le t \le T \tag{5c}$$

Then, the pressure in the storage tanks is given by,

$$H(t) = H_{min} + \left(\frac{H_{max} - H_{min}}{\rho_{max} - \rho_{min}}\right)[\rho(t) - \rho_{min}] \quad 0 \le t \le T \tag{6}$$

At time t, the battery bank can receive power from two sources: $P_{PB}(t)$ kW from the PV farm and $P_{GB}(t)$ kW from the local grid. Simultaneously, it can give power to two entities: P_{BE} kW to the WE cluster, and P_{BG} kW to the local grid. In addition, it may lose power due to self-discharge. The battery bank uses J types of battery storage systems (BSS). Each BSS j has U_j batteries of type j ($j = 1,2,\cdots,J$), where η_{cj} is the charging efficiency, η_{dj} is the discharging efficiency, and η_{lj} is loss coefficient of battery type j. Then, the energy balance for BSS j is,

$$\frac{dQ_{Bj}(t)}{dt} = \eta_{cj}P_{Bcj}(t) - \frac{P_{Bdj}(t)}{\eta_{dj}} - \eta_{lj}Q_{Bj}(t) \quad 0 \le t \le T, 1 \le j \le J \tag{7a}$$

$$Q_{Bj}(0) = Q_{Bj}(T) = Q_{Bj0} \quad 1 \le j \le J \tag{7b}$$

where,$Q_{Bj}(t)$ kWh is the energy stored in the BSS j at time t, $P_{Bcj}(t)$ is the power received and $P_{Bdj}(t)$ is the power dispensed by the BSS at time t. For any battery type j, these two power transfers and energy stored are limited by its specifications as stated below,

$$P_{Bcj}(t) \le U_j P^*_{Bcj} \quad 0 \le t \le T, 1 \le j \le J \tag{8a}$$

$$P_{Bdj}(t) \le U_j P^*_{Bdj} \quad 0 \le t \le T, 1 \le j \le J \tag{8b}$$

$$Q_{Bj}(t) \le U_j Q^*_{Bj}(t) \quad 0 \le t \le T, 1 \le j \le J \tag{8c}$$

The total power received by the battery bank must be distributed to the individual BSSs as follows,

$$P_{PB}(t) + P_{GB}(t) = \sum\nolimits_{j=1}^{J} P_{Bcj}(t) \quad 0 \le t \le T \tag{9a}$$

Similarly, the total power dispensed by the battery bank must come from the individual BSSs as follows,

$$P_{BE}(t) + P_{BG}(t) = \sum\nolimits_{j=1}^{J} P_{Bdj}(t) \quad 0 \le t \le T \tag{9b}$$

In practice, the export and import of power from and to the local grid are usually regulated to ensure grid stability. Therefore, the following user-specified limits must be imposed.

$$P_{GE}(t) + P_{GB}(t) \le P^*_{IMP}(t) \quad 0 \le t \le T \tag{10a}$$

$$P_{BG}(t) + P_{PG}(t) \le P^*_{EXP}(t) \quad 0 \le t \le T \tag{10b}$$

In addition to an energy balance for each individual unit of the facility, an overall energy balance over the entire facility can also be written. Considering potential energy losses in the battery bank, one can say that the total amount of energy into the facility (electricity produced by the solar PV farm and imported from the grid) must exceed the energy leaving the facility (hydrogen energy sold to the market and electricity exported to the grid) as follows.

$$\int_{t=0}^{T}\left[P_{GE}(t) + P_{GB}(t) + \sum\nolimits_{i=1}^{I}\alpha_i N_i IR(t)\right]dt \ge \int_{t=0}^{T}\left[P_{PG}(t) + P_{BG}(t) + \sum\nolimits_{s=1}^{S} P_{Es}(t)\right]dt \tag{11}$$

Although Eq. (11) is redundant, its addition may speed up the numerical solution of this optimization model.

Total land footprint and land cost are critical considerations for a facility to produce solar hydrogen. Its land footprint (*LFP*) must not exceed the available plot area,

$$LFP = \lambda_P \sum\nolimits_{i=1}^{I} N_i A_{Pi} + \lambda_E \sum\nolimits_{s=1}^{S} M_s A_{Es} + \lambda_{ST} \bullet NC \bullet L_{ST} \bullet D_{ST} + \lambda_B \sum\nolimits_{j=1}^{J} U_j A_{Bj} \tag{12a}$$

$$LFP \le A^* \tag{12b}$$

where, the λ's represent the land footprint multipliers, A's represent the areas for various components as defined in Section 3, L_{ST} is the length of horizontal hydrogen tanks, and D_{ST} is their diameter. Eq. (12a) also assumes that the hydrogen tanks are horizontal as stated in Section 3.

If $ps(t)$ is the price ($/kWh) at which the facility sells power to the local grid, and $pb(t)$ is the price ($/kWh) at which the facility buys power from the local grid, then the net revenue from electricity sales is,

$$REV = \int_0^T [ps(t)\{P_{BG}(t) + P_{PG}(t)\} - pb(t)\{P_{GB}(t) + P_{GE}(t)\}]dt \tag{13}$$

Furthermore, the grid electricity may have CO_2 emissions that are needed for carbon tax calculations. If $pc(t)$ is the carbon tax ($/tonne CO_{2eq}) and EI (tonne CO_{2eq}/kWh) is the grid emission intensity, then the annual carbon tax payable is given as,

$$CTAX = EI \int_0^T [pc(t)\{P_{GB}(t) + P_{GE}(t)\}]dt \tag{14}$$

The pumping station must supply 9 kg of water per kg of hydrogen to the WE cluster. While the model assumes them to be zero, the costs of water, water pump, and pumping energy can be computed from the optimal profiles of hydrogen production and stack pressure.

The annual Total Ownership Cost (*TOC*) or Total Annualized Cost (*TAC*) for the facility is estimated as follows. First, the total capital expenditure (*CAPEX*) for the facility is given by,

$$CAPEX(\$) = \sum\nolimits_{i=1}^{I} N_i C_{Pi} + \sum\nolimits_{s=1}^{S} M_s C_{Es} + \sum\nolimits_{j=1}^{J} U_j C_{Bj} + NC \bullet C_{ST} \tag{15a}$$

Note that,C's represent the CAPEX factors of various components as defined in Section 3. If a's represent the annualization factors for the capital costs of various components, then the annualized capital expense (*ACAPEX* $/y) is given by,

$$ACAPEX = a_P \sum_{i=1}^{I} N_i C_{Pi} + a_E \sum_{s=1}^{S} M_s C_{Es} + a_B \sum_{j=1}^{J} U_j C_{Bj} + a_{ST} \bullet NC \bullet C_{ST} \tag{15b}$$

Now, the following *TAC* for producing hydrogen is minimized.

$$\begin{aligned} Minimize \quad & TAC = ACAPEX + fopexCAPEX \\ & + C_L LFP - REV + CTAX \end{aligned} \tag{16}$$

$$LCOH = \frac{TAC}{1000 \int_0^T D(t)dt} \$ \Big/ kgH_2 \tag{17}$$

Eq. 1–17 define an optimization problem for designing the solar hydrogen facility. It is a mixed integer nonlinear programming problem, where M_s, N_i, U_j, and *NC* are discrete, and all others are continuous variables. While the problem formulation does not explicitly limit the total carbon emissions, Eq. (14) limits the amount of grid power use, and hence indirectly limits the emissions. In other words, the limit on the grid power import dictates the carbon emissions incurred in the hydrogen production.

Appendix C:. Solution approach

The facility design problem formulated above involves algebraic, differential, and integral equations. Typical public profiles for irradiance and electricity prices are at discrete intervals (*e.g.* 30 min in Singapore). Hence, the year is discretized into *K* intervals ($k = 1, 2, \cdots, K; K = 8784/h$ for a leap year; $K = 8760/h$ otherwise) of *h* hour each and convert Eqs. (1–17) into their discrete finite difference forms. An interval *k* begins at $t = T_{k-1} = (k-1)h$. All variables in Eqs. (1–17) will now be defined at discrete points $t = T_k$ ($k = 0, 1, \cdots, K$). Then, letting $IR_k = IR(T_k)$, $P_{PEk} = P_{PE}(T_k)$, $P_{PBk} = P_{PB}(T_k)$, $P_{PGk} = P_{PG}(T_k)$, $P_{GEk} = P_{GE}(T_k)$, $P_{GBk} = P_{GB}(T_k)$, $P_{BEk} = P_{BE}(T_k)$, $P_{BGk} = P_{BG}(T_k)$, $P_{Esk} = P_{Es}(T_k)$, $\rho_k = \rho(T_k)$, $H_k = H(T_k)$, $D_k = D(T_k)$, $Q_{Bjk} = Q_{Bj}(T_k)$, $P_{Bcjk} = P_{Bcj}(T_k)$, $P_{Bdjk} = P_{Bdj}(T_k)$, $ps_k = ps(T_k)$, $pb_k = pb(T_k)$, and $pc_k = pc(T_k)$, $P^*_{EXPk} = P^*_{EXP}(T_k)$, and $P^*_{IMPk} = P^*_{IMP}(T_k)$, Eqs. (1–17) are rewritten as,

$$\sum_{i=1}^{I} \alpha_i N_i IR_k \geq P_{PEk} + P_{PBk} + P_{PGk} \qquad 0 \leq k \leq K \tag{18}$$

$$P_{PEk} + P_{GEk} + P_{BEk} \geq \sum_{s=1}^{S} P_{Esk} \qquad 0 \leq k \leq K \tag{19a}$$

$$P_{Esk} \leq M_s P^*_{Es} \qquad 0 \leq k \leq K, 1 \leq s \leq S \tag{19b}$$

$$NC \bullet V\rho_{(k+1)} = NC \bullet V\rho_k + \frac{h}{2}\left[\left\{\sum_{s=1}^{S} \frac{R^*_{Es}}{P^*_{Es}}\left(P_{Es(k+1)} + P_{Esk}\right)\right\} - \left(D_{(k+1)} + D_k\right)\right] \qquad 0 \leq k < K \tag{20a}$$

$$\rho_K = \rho_0 \tag{20b}$$

$$\rho_{min} \leq \rho_k \leq \rho_{max} \qquad 0 \leq k \leq K \tag{20c}$$

$$H_k = H_{min} + \left(\frac{H_{max} - H_{min}}{\rho_{max} - \rho_{min}}\right)\{\rho_k - \rho_{min}\} \qquad 0 \leq k \leq K \tag{21a}$$

$$H_{min} \leq H_k \leq H_{max} \qquad 0 \leq k \leq K \tag{21b}$$

$$Q_{Bj(k+1)} = Q_{Bjk} + \frac{h}{2}\left[\begin{array}{c} \eta_{cj}\left(P_{Bcj(k+1)} + P_{Bcjk}\right) - \frac{1}{\eta_{dj}}\left(P_{Bdj(k+1)} + P_{Bdjk}\right) \\ -\eta_{lj}\left(Q_{Bj(k+1)} + Q_{Bjk}\right) \end{array}\right] \qquad 0 \leq k < K \tag{22a}$$

$$Q_{BK} = Q_{B0} \tag{22b}$$

$$P_{Bcjk} \leq U_j P^*_{Bj} \qquad 0 \leq k \leq K, 1 \leq j \leq J \tag{23a}$$

$$P_{Bdjk} \leq U_j P^*_{Bj} \qquad 0 \leq k \leq K, 1 \leq j \leq J \tag{23b}$$

$$Q_{Bjk} \leq U_j Q^*_{Bj} \qquad 0 \leq k \leq K, 1 \leq j \leq J \tag{23c}$$

$$P_{PBk} + P_{GBk} = \sum_{j=1}^{J} P_{Bcjk} \qquad 0 \leq k \leq K \tag{24a}$$

$$P_{BEk} + P_{BGk} = \sum_{j=1}^{J} P_{Bdjk} \qquad 0 \leq k \leq K \tag{24b}$$

$$P_{GEk} + P_{GBk} \leq P^*_{IMPk} \qquad 0 \leq k \leq K \tag{25a}$$

$$P_{BGk} + P_{PGk} \leq P^*_{EXPk} \qquad 0 \leq k \leq K \tag{25b}$$

$$\sum_{k=0}^{K-1}\sum_{i=1}^{I}\alpha_i N_i[IR_{k+1}+IR_k]+\sum_{k=0}^{K-1}\left[P_{GE(k+1)}+P_{GEk}+P_{GB(k+1)}+P_{GBk}\right]\geq \sum_{k=0}^{K-1}\sum_{s=1}^{S}\left(P_{Es(k+1)}+P_{Esk}\right)+\sum_{k=0}^{K-1}\left[P_{PG(k+1)}+P_{PGk}+P_{BG(k+1)}+P_{BGk}\right] \tag{26}$$

$$\lambda_P\sum_{i=1}^{I}N_iA_{Pi}+\lambda_E\sum_{s=1}^{S}M_sA_{Es}+\lambda_{ST}\bullet NC\bullet L_{ST}D_{ST}+\lambda_B\sum_{j=1}^{J}U_jA_{Bj}\leq A^{*} \tag{27}$$

$$Minimize \quad TAC=\left\{\begin{array}{l}\left[a_P\sum_{i=1}^{I}N_iC_{Pi}+a_E\sum_{s=1}^{S}M_sC_{Es}+a_B\sum_{j=1}^{J}U_jC_{Bj}+a_{ST}\bullet NC\bullet C_{ST}\right]+\\ fopex\left[\sum_{i=1}^{I}N_iC_{Pi}+\sum_{s=1}^{S}M_sC_{Es}+\sum_{j=1}^{J}U_jC_{Bj}+NC\bullet C_{ST}\right]+\\ C_L\left[\lambda_P\sum_{i=1}^{I}N_iA_{Pi}+\lambda_E\sum_{s=1}^{S}M_sA_{Es}+\lambda_{ST}\bullet NC\bullet L_{ST}D_{ST}+\lambda_B\sum_{j=1}^{J}U_jA_{Bj}\right]-\\ \frac{h}{2}\sum_{k=0}^{K-1}\left[\begin{array}{l}ps_k\left\{P_{BGk}+P_{BG(k+1)}+P_{PGk}+P_{PG(k+1)}\right\}\\ -pb_k\left\{P_{GBk}+P_{GB(k+1)}+P_{GEk}+P_{GE(k+1)}\right\}\end{array}\right]+\\ \frac{h\times EI}{2}\sum_{k=0}^{K-1}pc_k\left\{P_{GBk}+P_{GB(k+1)}+P_{GEk}+P_{GE(k+1)}\right\}\end{array}\right\}$$

The discretized model is written in GAMS (General Algebraic Modelling System) and solved using the commercial MINLP solver called BARON. The case studies are executed on Dell Precision 7920 workstation with Intel Xeon® Platinum 8168 CPU, 24 cores, and 128 GB RAM.

References

[1] Oyewunmi T. Resilience, reliability and gas to power systems in the USA: an energy policy outlook in the era of decarbonization. J World Energy Law Business 2021; 14:257–76.
[2] Elavarasan RM, Pugazhendhi R, Irfan M, Mihet-Popa L, Khan IA, Campana PE. State-of-the-art sustainable approaches for deeper decarbonization in Europe–An endowment to climate neutral vision. Renew Sustain Energy Rev 2022;159: 112204.
[3] Buira D, Tovilla J, Farbes J, Jones R, Haley B, Gastelum D. A whole-economy deep decarbonization pathway for Mexico. Energ Strat Rev 2021;33:100578.
[4] Luo S, Hu W, Liu W, Xu X, Huang Q, Chen Z, et al. Transition pathways towards a deep decarbonization energy system—A case study in Sichuan, China. Appl Energy 2021;302:117507.
[5] Hong X, Thaore VB, Garud SS, Karimi IA, Farooq S, Wang X, et al. Decarbonizing Singapore via local production of H2 from natural gas. Int J Hydrogen Energy 2022.
[6] Dong ZY, Yang J, Yu L, Daiyan R, Amal R. A green hydrogen credit framework for international green hydrogen trading towards a carbon neutral future. Int J Hydrogen Energy 2022;47:728–34.
[7] Sy O, Li J. Evaluation of the introduction of a hydrogen supply chain using a conventional gas pipeline–A case study of the Qinghai-Shanghai hydrogen supply chain. Int J Hydrogen Energy 2020;45:33846–59.
[8] Hong X, Thaore VB, Karimi IA, Farooq S, Wang X, Usadi AK, et al. Techno-enviro-economic analyses of hydrogen supply chains with an ASEAN case study. Int J Hydrogen Energy 2021;46:32914–28.
[9] Gu Y, Chen Q, Xue J, Tang Z, Sun Y, Wu Q. Comparative techno-economic study of solar energy integrated hydrogen supply pathways for hydrogen refueling stations in China. Energ Conver Manage 2020;223:113240.
[10] Temiz M, Dincer I. Techno-economic analysis of green hydrogen ferries with a floating photovoltaic based marine fueling station. Energ Conver Manage 2021; 247:114760.
[11] Life RR. Cycle Emissions of Hydrogen 2020. https://4thgeneration.energy/life-cycles-emissions-of-hydrogen/.
[12] Ishaq H, Dincer I, Crawford C. A review on hydrogen production and utilization: Challenges and opportunities. Int J Hydrogen Energy 2022;47:26238–64.
[13] Guban D, Muritala IK, Roeb M, Sattler C. Assessment of sustainable high temperature hydrogen production technologies. Int J Hydrogen Energy 2020;45: 26156–65.
[14] Boretti A. There are hydrogen production pathways with better than green hydrogen economic and environmental costs. Int J Hydrogen Energy 2021;46: 23988–95.
[15] Nikolaidis P, Poullikkas A. A comparative overview of hydrogen production processes. Renew Sustain Energy Rev 2017;67:597–611.
[16] Grigoriev S, Fateev V, Bessarabov D, Millet P. Current status, research trends, and challenges in water electrolysis science and technology. Int J Hydrogen Energy 2020;45:26036–58.
[17] Schmidt O, Gambhir A, Staffell I, Hawkes A, Nelson J, Few S. Future cost and performance of water electrolysis: An expert elicitation study. Int J Hydrogen Energy 2017;42:30470–92.
[18] Burke J. 'Green' hydrogen price dropping faster than expected. BloombergNEF 2021. https://www.dieselgasturbine.com/news/-Green-hydrogen-price-dropping-faster-than-expected-BloombergNEF/8011420.article.
[19] Hong X, Garud SS, Thaore VB, Karimi IA, Farooq S, Wang X, et al. Hydrogen Economy Assessment & Resource Tool (HEART): A python-based tool for ASEAN H2 roadmap study. Int J Hydrogen Energy 2022;47:21897–907.
[20] Kakoulaki G, Kougias I, Taylor N, Dolci F, Moya J, Jäger-Waldau A. Green hydrogen in Europe–A regional assessment: Substituting existing production with electrolysis powered by renewables. Energ Conver Manage 2021;228:113649.
[21] Ligen Y, Vrubel H, Girault H. Energy efficient hydrogen drying and purification for fuel cell vehicles. Int J Hydrogen Energy 2020;45:10639–47.
[22] Nami H, Rizvandi OB, Chatzichristodoulou C, Hendriksen PV, Frandsen HL. Techno-economic analysis of current and emerging electrolysis technologies for green hydrogen production. Energ Conver Manage 2022;269:116162.
[23] Jang D, Kim J, Kim D, Han W-B, Kang S. Techno-economic analysis and Monte Carlo simulation of green hydrogen production technology through various water electrolysis technologies. Energ Conver Manage 2022;258:115499.
[24] Jang D, Kim K, Kim K-H, Kang S. Techno-economic analysis and Monte Carlo simulation for green hydrogen production using offshore wind power plant. Energ Conver Manage 2022;263:115695.
[25] Manzotti A, Quattrocchi E, Curcio A, Kwok SC, Santarelli M, Ciucci F. Membraneless electrolyzers for the production of low-cost, high-purity green hydrogen: A techno-economic analysis. Energ Conver Manage 2022;254:115156.
[26] Biggins F, Kataria M, Roberts D, Brown S. Green hydrogen investments: Investigating the option to wait. Energy 2022;241:122842.
[27] Na J, Seo B, Kim J, Lee CW, Lee H, Hwang YJ, et al. General technoeconomic analysis for electrochemical coproduction coupling carbon dioxide reduction with organic oxidation. Nat Commun 2019;10:5193.
[28] Astakhov O, Agbo S, Welter K, Smirnov V, Rau U, Merdzhanova T. Storage batteries in photovoltaic–electrochemical device for solar hydrogen production. J Power Sources 2021;509:230367.
[29] Zurita A, Mata-Torres C, Valenzuela C, Felbol C, Cardemil JM, Guzmán AM, et al. Techno-economic evaluation of a hybrid CSP+ PV plant integrated with thermal energy storage and a large-scale battery energy storage system for base generation. Sol Energy 2018;173:1262–77.
[30] Tawarmalani M, Sahinidis NV. A polyhedral branch-and-cut approach to global optimization. Math Program 2005;103:225–49.
[31] NASA Langley Research Centre 2022. https://power.larc.nasa.gov/data-access-viewer/.
[32] Marafiq 2023. https://www.marafiq.com.sa/en/partnering-with-us/water-tariff/.
[33] PowerWater 2023. https://www.powerwater.com.au/customers/water-and-wastewater/my-water-bill/water-pricing-and-tariffs.
[34] Water Price. PUB 2023. https://www.pub.gov.sg/watersupply/waterprice.
[35] Europe 2021. https://www.waternewseurope.com/water-prices-compared-in-36-eu-cities/.
[36] Cole WJ, Frazier A. Cost projections for utility-scale battery storage. National Renewable Energy Lab. (NREL), Golden, CO (United States) 2019.